Supporting information for the paper entitled:

Phenylimido Complexes of Rhenium: Fluorine Substituents Provide Protection, Reactivity and Solubility

Guilhem Claude,[a] Erika Kulitzki,[a] Adelheid Hagenbach,[a] Maximilian Roca Jungfer,[a] Joshua R. Figueroa[b], and Ulrich Abram[a*]*

[a]Freie Universität Berlin, Institute of Chemistry and Biochemistry, Fabeckstr. 34–36, 14195 Berlin, Germany

E-mail: ulrich.abram@fu-berlin.de

[b]Department of Chemistry and Biochemistry, University of California, San Diego, La Jolla, California 92093, United States

E-mail: jsfig@ucsd.edu

Table of content

Crystallographic data

The intensities for the X–ray determinations were collected on STOE IPDS 2T with Mo Kα radiation. The space groups were determined by the detection of systematical absences. Absorption corrections were carried out by integration methods.[1] Structure solution and refinement were performed with the SHELX program package.[2,3] Hydrogen atoms were derived from the final Fourier maps and refined or placed at calculated positions and treated with the 'riding model' option of SHELXL. The representation of molecular structures was done using the program DIAMOND 4.2.2.[4]
Additional information on the structure determinations has been deposited with the Cambridge Crystallographic Data Centre.

Table S1: Crystallographic data and data collection parameters

	$[Re(NPhF)Cl_3(PPh_3)(CN^tBu)]$ (**2**)	$[Re(NPhF)Cl_3(PPh_3)(CNPh)]$ (**3**)	$[Re(NPhF)Cl_3(PPh_3)(CNPh^{i\text{-}prop2})]$ (**4**)
Empirical formula	$C_{29}H_{28}Cl_3FN_2PRe$	$C_{31}H_{24}Cl_3FN_2PRe$	$C_{37}H_{36}Cl_3FN_2PRe$
Formula weight	747.05	767.04	851.20
Temperature/K	200.0	100.0	200
Crystal system	triclinic	monoclinic	monoclinic
Space group	$P\bar{1}$	$P2_1/c$	$P2_1/c$
a/Å	10.2945(6)	12.4219(9)	18.349(4)
b/Å	14.5070(8)	11.5944(8)	10.552(2)
c/Å	21.6560(1)	20.6804(2)	19.299(4)
α/°	70.369(4)	90	90
β/°	83.840(5)	106.880(3)	99.46(3)
γ/°	89.494(5)	90	90
Volume/Å^3	3027.3(3)	2850.2(4)	3686.1(1)
Z	4	4	4
ρ_{calc}g / cm^3	1.639	1.788	1.534
μ / mm^{-1}	4.358	4.632	3.590
F(000)	1464.0	1496.0	1688.0
Crystal size / mm^3	0.28 × 0.17 × 0.08	0.21 × 0.18 × 0.04	0.58 × 0.35 × 0.13
Radiation	MoKα (λ = 0.71073)	MoKα (λ = 0.71073)	Mo Kα (λ = 0.71073)
2Θ range for data collection/°	6.69 to 52.154	4.528 to 54.274	6.702 to 51.998
Index ranges	-12 ≤ h ≤ 12, -17 ≤ k ≤ 16, -26 ≤ l ≤ 26	-15 ≤ h ≤ 15, -14 ≤ k ≤ 14, -26 ≤ l ≤ 26	-22 ≤ h ≤ 22, -12 ≤ k ≤ 12, -23 ≤ l ≤ 23
Reflections collected	25804	49900	26788
Independent reflections	11870 [R_{int} = 0.0368, R_{sigma} = 0.0481]	6252 [R_{int} = 0.0354, R_{sigma} = 0.0196]	7171 [R_{int} = 0.0401, R_{sigma} = 0.0309]
Data/restraints/parameters	11870/0/667	6252/0/352	7171/500/410
Goodness-of-fit on F^2	0.888	1.141	0.979
Final R indexes [I>=2σ (I)]	R_1 = 0.0235, wR_2 = 0.0411	R_1 = 0.0268, wR_2 = 0.0564	R_1 = 0.0252, wR_2 = 0.0541
Final R indexes [all data]	R_1 = 0.0413, wR_2 = 0.0439	R_1 = 0.0288, wR_2 = 0.0571	R_1 = 0.0358, wR_2 = 0.0565
Largest diff. peak/hole / e Å^{-3}	0.53/-0.78	2.53/-1.21	0.57/-0.97
Flack	–	–	–
Diffractometer	IPDS 2T	D8 Venture	IPDS 2T
CCDC access code	2236802	2236803	2236804

Table S1 (continued): Crystallographic data and data collection parameters.

	[Re(NPhF)Cl_3(PPh_3)(CNMes)] (**5**)	[Re(NPhF)Cl_3(PPh_3)(CNPh^{pNO2})] (**6**)	[Re(NPhF)Cl_3(CNAr^{Mes2})$_2$] x 1.5 toluene (**7**)
Empirical formula	$C_{34}H_{30}Cl_3FN_2PRe$	$C_{31}H_{23}Cl_3FN_3O_2PRe$	$C_{66.5}H_{66}Cl_3FN_3Re$
Formula weight	809.12	812.04	1218.77
Temperature/K	200	200	200.0
Crystal system	monoclinic	monoclinic	triclinic
Space group	$P2_1/n$	$P2_1/c$	$P\bar{1}$
a/Å	9.6268(7)	9.0634(2)	12.5541(7)
b/Å	20.7312(1)	25.461(5)	13.5237(7)
c/Å	16.4187(1)	13.352(3)	20.8711(1)
α/°	90	90	77.386(4)
β/°	100.002(5)	99.20(3)	86.283(4)
γ/°	90	90	64.117(4)
Volume / Å^3	3227.0(3)	3041.4(11)	3109.2(3)
Z	4	4	2
ρ_{calc} g/cm^3	1.665	1.773	1.302
μ / mm^{-1}	4.096	4.352	2.118
F(000)	1592.0	1584.0	1242
Crystal size / mm^3	0.31 × 0.143 × 0.02	0.33 × 0.157 × 0.03	0.3 × 0.2 × 0.2
Radiation	Mo Kα (λ = 0.71073)	Mo Kα (λ = 0.71073)	MoKα (λ = 0.71073)
2Θ range for data collection/°	6.636 to 51.996	6.618 to 52	6.672 to 51.998
Index ranges	-10 ≤ h ≤ 11, -25 ≤ k ≤ 25, -20 ≤ l ≤ 20	-11 ≤ h ≤ 11, -31 ≤ k ≤ 31, -16 ≤ l ≤ 15	-14 ≤ h ≤ 15, -15 ≤ k ≤ 16, -25 ≤ l ≤ 25
Reflections collected	18114	17337	25031
Independent reflections	6313 [R_{int} = 0.0394, R_{sigma} = 0.0452]	5953 [R_{int} = 0.0637, R_{sigma} = 0.0749]	12158 [R_{int} = 0.0674, R_{sigma} = 0.0614]
Data/restraints/parameters	6313/0/382	5953/0/379	12158/0/578
Goodness-of-fit on F^2	0.919	0.822	0.961
Final R indexes [I>=2σ (I)]	R_1 = 0.0271, wR_2 = 0.0470	R_1 = 0.0281, wR_2 = 0.0423	R_1 = 0.0368, wR_2 = 0.0873
Final R indexes [all data]	R_1 = 0.0458, wR_2 = 0.0501	R_1 = 0.0568, wR_2 = 0.0459	R_1 = 0.0459, wR_2 = 0.0901
Largest diff. peak/hole / e Å^{-3}	0.54/-1.07	0.56/-0.70	1.19/-1.15
Flack	–	–	–
Diffractometer	IPDS 2T	IPDS 2T	IPDS 2T
CCDC access code	2236805	2236806	2236807

Table S1 (continued): Crystallographic data and data collection parameters.

	$[Re(NPhF)Cl_3(CNAr^{Dipp2})_2]$ (**8**) + 0.5 CH_2Cl_2 +1.25 toluene*	$[Re(NPhF)Cl_3(PPh_3)(CNAr^{Tripp2})]$ (**9**)+ THF	$[Re(NPhF)Cl_3(CNAr^{Tripp2})_2]$ (**10**)
Empirical formula	$C_{154.5}H_{178}Cl_8F_2N_6Re_2$	$C_{65}H_{76}Cl_3FN_2OPRe$	$C_{80}H_{102}Cl_3FN_3Re$
Formula weight	2813.02	1243.79	1417.19
Temperature/K	100	200	200
Crystal system	triclinic	triclinic	monoclinic
Space group	P1	$P\bar{1}$	$P2_1/n$
a/Å	14.706(3)	10.858(2)	24.4087(9)
b/Å	16.346(3)	14.422(3)	25.0277(7)
c/Å	17.419(5)	20.631(4)	28.2885(1)
α/°	84.392(8)	77.64(3)	90
β/°	82.455(9)	75.03(3)	108.962(3)
γ/°	63.855(5)	81.35(3)	90
Volume / $Å^3$	3722.5(2)	3033.2(1)	16343.5(1)
Z	1	2	8
ρ_{calc} g/cm^3	1.255	1.362	1.152
μ / mm^{-1}	1.820	2.206	1.626
F(000)	1451.0	1276.0	5904.0
Crystal size / mm^3	0.24 × 0.21 × 0.18	0.32 × 0.143 × 0.05	0.9 × 0.5 × 0.5
Radiation	MoKα (λ = 0.71073)	Mo Kα (λ = 0.71073)	Mo Kα (λ = 0.71073)
2Θ range for data collection/°	4.722 to 55.978	6.73 to 52	6.618 to 52
Index ranges	-19 ≤ h ≤ 19, -21 ≤ k ≤ 21, -22 ≤ l ≤ 22	-13 ≤ h ≤ 13, -17 ≤ k ≤ 17, -25 ≤ l ≤ 25	-30 ≤ h ≤ 30, -30 ≤ k ≤ 30, -34 ≤ l ≤ 34
Reflections collected	167349	25108	107340
Independent reflections	35322 [R_{int} = 0.0455, R_{sigma} = 0.0472]	11861 [R_{int} = 0.0721, R_{sigma} = 0.1409]	32003 [R_{int} = 0.0901, R_{sigma} = 0.1020]
Data/restraints/parameters	35322/1904/1479	11861/0/679	32003/2108/1595
Goodness-of-fit on F^2	1.045	0.755	0.881
Final R indexes [I>=2σ (I)]	R_1 = 0.0396, wR_2 = 0.0993	R_1 = 0.0417, wR_2 = 0.0551	R_1 = 0.0524, wR_2 = 0.1164
Final R indexes [all data]	R_1 = 0.0460, wR_2 = 0.1039	R_1 = 0.0810, wR_2 = 0.0618	R_1 = 0.1130, wR_2 = 0.1346
Largest diff. peak/hole / e $Å^{-3}$	1.74/-1.49	0.69/-0.65	1.17/-1.51
Flack	0.009(2)	–	–
Diffractometer	D8 Venture	IPDS 2T	IPDS 2T
CCDC access code	2236808	2236809	2236810

*The unusual space group P1 has been checked for higher symmetry by several methods, but no inversion center has been found.

Table S1 (continued): Crystallographic data and data collection parameters.

	$[Re(NPhF)Cl_3(PPh_3)(CNp\text{-}FAr^{DarF2})]$ x 0.5 CH_2Cl_2 (**11**)	$[Re(NPhF)Cl_3(PPh_3)(CNPh^{pF})]$ (**12**)
Empirical formula	$C_{47}H_{27}Cl_3F_{14}N_2PRe$	$C_{31}H_{23}Cl_3F_2N_2PRe$
Formula weight	1209.22	785.03
Temperature/K	105.0	200
Crystal system	tetragonal	monoclinic
Space group	$I4_1/a$	$P2_1/n$
a/Å	46.9293(1)	11.170(2)
b/Å	46.9293(1)	21.178(4)
c/Å	8.3649(2)	12.895(3)
α/°	90	90
β/°	90	103.82(3)
γ/°	90	90
Volume / $Å^3$	18422.5(9)	2962.1(1)
Z	16	4
ρ_{calc} g/cm^3	1.744	1.760
μ / mm^{-1}	7.935	4.464
F(000)	9440.0	1528.0
Crystal size / mm^3	0.15 × 0.1 × 0.08	0.21 × 0.07 × 0.027
Radiation	CuKα (λ = 1.54178)	MoKα (λ = 0.71073)
2Θ range for data collection/°	5.326 to 133.24	6.626 to 52.016
Index ranges	-55 ≤ h ≤ 55, -55 ≤ k ≤ 55, -9 ≤ l ≤ 9	-13 ≤ h ≤ 13, -26 ≤ k ≤ 26, -14 ≤ l ≤ 15
Reflections collected	173200	17347
Independent reflections	8121 [R_{int} = 0.0672, R_{sigma} = 0.0185]	5800 [R_{int} = 0.0596, R_{sigma} = 0.0714]
Data/restraints/parameters	8121/6/633	5800/0/362
Goodness-of-fit on F^2	1.030	0.886
Final R indexes [I>=2σ (I)]	R_1 = 0.0287, wR_2 = 0.0703	R_1 = 0.0358, wR_2 = 0.0597
Final R indexes [all data]	R_1 = 0.0332, wR_2 = 0.0734	R_1 = 0.0663, wR_2 = 0.0652
Largest diff. peak/hole / e $Å^{-3}$	1.48/-0.96	1.44/-1.26
Flack	–	–
Diffractometer	D8 Venture	IPDS 2T
CCDC access code	2236811	2236812

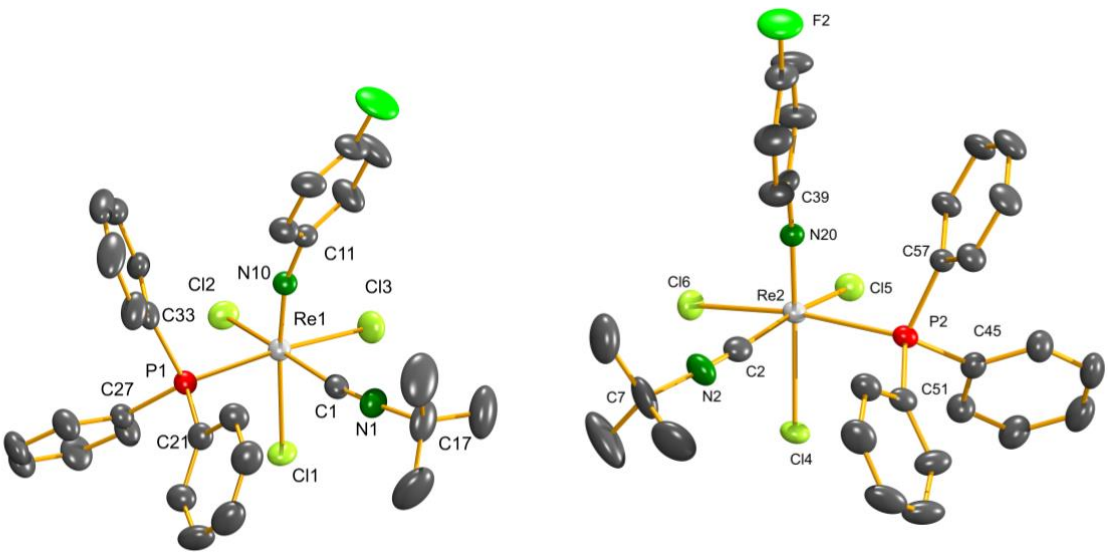

Figure S1: Ellipsoid representation of [Re(NPhF)Cl_3(PPh_3)(CN^tBu)] (**2**). The thermal ellipsoids are set at a 50% probability level. Hydrogen atoms are omitted for clarity.

Table S2A: Selected bond lengths (Å) and angles (°) in [Re(NPhF)Cl_3(PPh_3)(CN^tBu)] (**2**).

Re1-Cl2	2.4252(10)	P1-C21	1.812(4)	Re1-Cl3	2.4252(10)
Re1-Cl1	2.3994(9)	P1-C27	1.829(3)	Re1-N10	1.715(3)
Re1-P1	2.4593(9)	P1-C33	1.830(3)	Re1-C1	2.020(4)
N10-C11	1.391(4)	C1-N1	1.151(5)	N1-C17	1.458(5)
Cl2-Re1-Cl1	91.91(3)	Cl1-Re1-P1	84.47(3)	C11-N10-Re1	164.4(3)
Cl2-Re1-P1	92.38(3)	Cl1-Re1-Cl3	89.43(4)	C1-Re1-P1	94.61(11)
Cl2-Re1-Cl3	86.06(4)	Cl3-Re1-P1	173.65(3)	N1-C1-Re1	172.9(3)
C1-Re1-Cl2	169.35(10)	C1-Re1-Cl1	80.79(9)	C1-N1-C17	175.7(4)

Table S2B: Selected bond lengths (Å) and angles (°) in [Re(NPhF)Cl_3(PPh_3)(CN^tBu)] (**2**).

Re2-Cl5	2.3887(9)	P2-C45	1.841(4)	Re2-Cl6	2.4144(9)
Re2-Cl4	2.4276(8)	P2-C51	1.816(3)	Re2-N20	1.715(3)
Re2-P2	2.4473(9)	P2-C57	1.818(3)	Re2-C2	2.045(4)
N20-C39	1.382(4)	C2-N2	1.146(5)	N2-C7	1.463(5)
Cl4-Re2-Cl5	92.15(3)	Cl4-Re2-P2	82.98(3)	C39-N20-Re2	166.7(2)
Cl5-Re2-P2	88.41(3)	Cl4-Re2-Cl6	87.77(3)	C2-Re2-P2	97.1(1)
Cl5-Re2-Cl6	85.87(3)	Cl6-Re2-P2	168.93(3)	N2-C2-Re2	173.8(3)
C2-Re2-Cl5	167.96(1)	C2-Re2-Cl4	78.03(1)	C2-N2-C7	167.6(4)

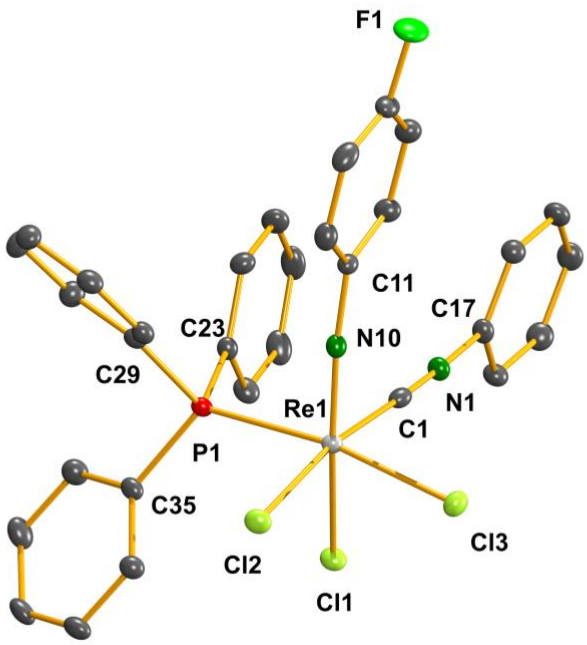

Figure S2: Ellipsoid representation of [Re(NPhF)Cl_3(PPh_3)(CNPh)] (**3**). The thermal ellipsoids are set at a 50% probability level. Hydrogen atoms are omitted for clarity.

Table S3: Selected bond lengths (Å) and angles (°) in [Re(NPhF)Cl_3(PPh_3)(CNPh)] (**3**).

Re1-Cl2	2.3921(9)	P1-C23	1.819(4)	Re1-Cl3	2.4254(9)
Re1-Cl1	2.4097(9)	P1-C29	1.828(4)	Re1-N10	1.730(3)
Re1-P1	2.4539(9)	P1-C35	1.830(4)	Re1-C1	2.029(4)
N10-C11	1.378(4)	C1-N1	1.165(5)	N1-C17	1.397(5)
Cl2-Re1-Cl1	92.29(3)	Cl1-Re1-P1	84.40(3)	C11-N10-Re1	168.7(3)
Cl2-Re1-P1	90.63(3)	Cl1-Re1-Cl3	87.00(3)	C1-Re1-P1	91.74(1)
Cl2-Re1-Cl3	85.46(3)	Cl3-Re1-P1	170.41(3)	N1-C1-Re1	177.7(3)
C1-Re1-Cl2	169.85(10)	C1-Re1-Cl1	91.74(10)	C1-N1-C17	177.7(4)

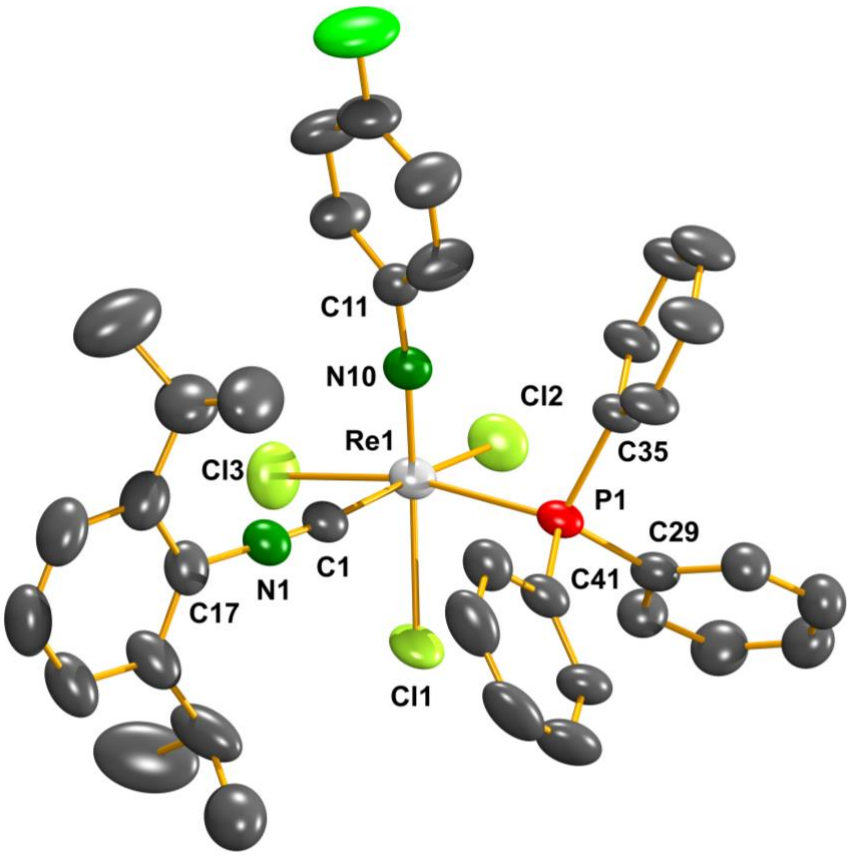

Figure S3: Ellipsoid representation of [Re(NPhF)Cl_3(PPh_3)(CNPh$^{i\text{-prop2}}$)] (**4**). The thermal ellipsoids are set at a 50% probability level. Hydrogen atoms are omitted for clarity.

Table S4: Selected bond lengths (Å) and angles (°) in [Re(NPhF)Cl_3(PPh_3)(CNPh$^{i\text{-prop2}}$)] (**4**).

Re1-Cl2	2.3946(1)	P1-C29	1.832(3)	Re1-Cl3	2.4144(10)
Re1-Cl1	2.4294(9)	P1-C35	1.821(3)	Re1-N10	1.722(3)
Re1-P1	2.4476(9)	P1-C41	1.823(3)	Re1-C1	2.023(3)
N10-C11	1.385(4)	C1-N1	1.147(4)	N1-C17	1.404(4)
Cl2-Re1-Cl1	93.93(4)	Cl1-Re1-P1	79.36(3)	C11-N10-Re1	172.1(2)
Cl2-Re1-P1	89.44(4)	Cl1-Re1-Cl3	86.88(4)	C1-Re1-P1	97.52(10)
Cl2-Re1-Cl3	86.71(4)	Cl3-Re1-P1	165.42(3)	N1-C1-Re1	170.6(3)
C1-Re1-Cl2	169.54(9)	C1-Re1-Cl1	79.78(9)	C1-N1-C17	172.6(3)

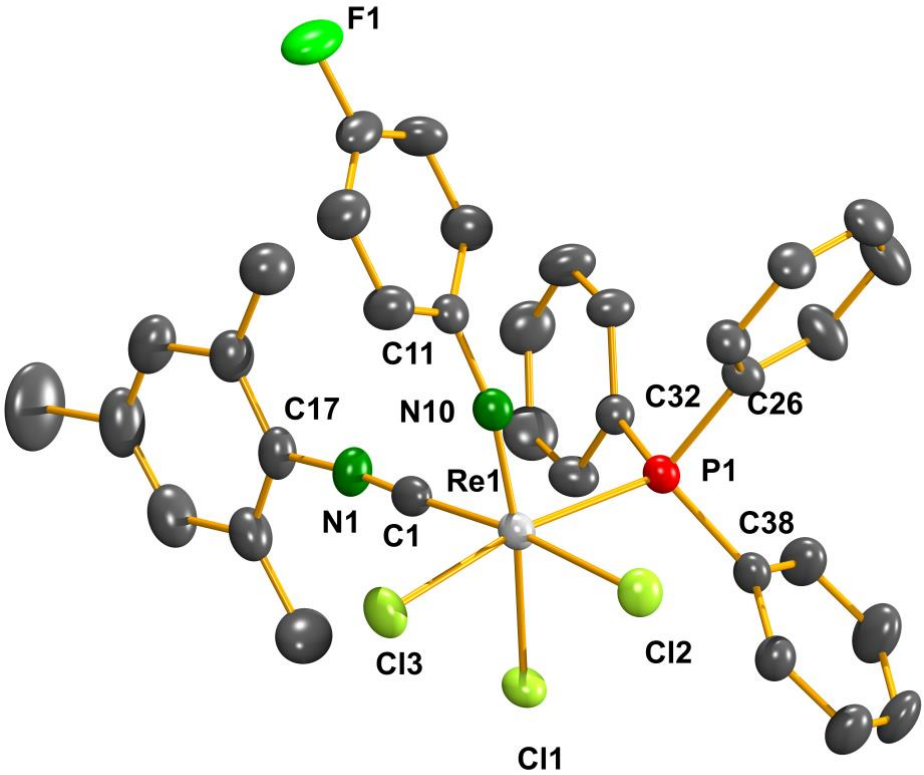

Figure S4: Ellipsoid representation of [Re(NPhF)Cl_3(PPh_3)(CNMes)] (**5**). The thermal ellipsoids are set at a 50% probability level. Hydrogen atoms are omitted for clarity.

Table S5: Selected bond lengths (Å) and angles (°) in [Re(NPhF)Cl_3(PPh_3)(CNMes)] (**5**).

Re1-Cl2	2.4034(1)	P1-C26	1.828(4)	Re1-Cl3	2.4345(9)
Re1-Cl1	2.3957(1)	P1-C32	1.815(4)	Re1-N10	1.712(3)
Re1-P1	2.4631(1)	P1-C38	1.828(4)	Re1-C1	2.030(4)
N10-C11	1.399(5)	C1-N1	1.151(5)	N1-C17	1.404(5)
Cl2-Re1-Cl1	92.88(4)	Cl1-Re1-P1	85.04(3)	C11-N10-Re1	166.0(3)
Cl2-Re1-P1	88.75(3)	Cl1-Re1-Cl3	88.05(4)	C1-Re1-P1	92.00(11)
Cl2-Re1-Cl3	86.53(4)	Cl3-Re1-P1	171.42(3)	N1-C1-Re1	176.9(3)
C1-Re1-Cl2	173.33(1)	C1-Re1-Cl1	80.58(11)	C1-N1-C17	174.1(4)

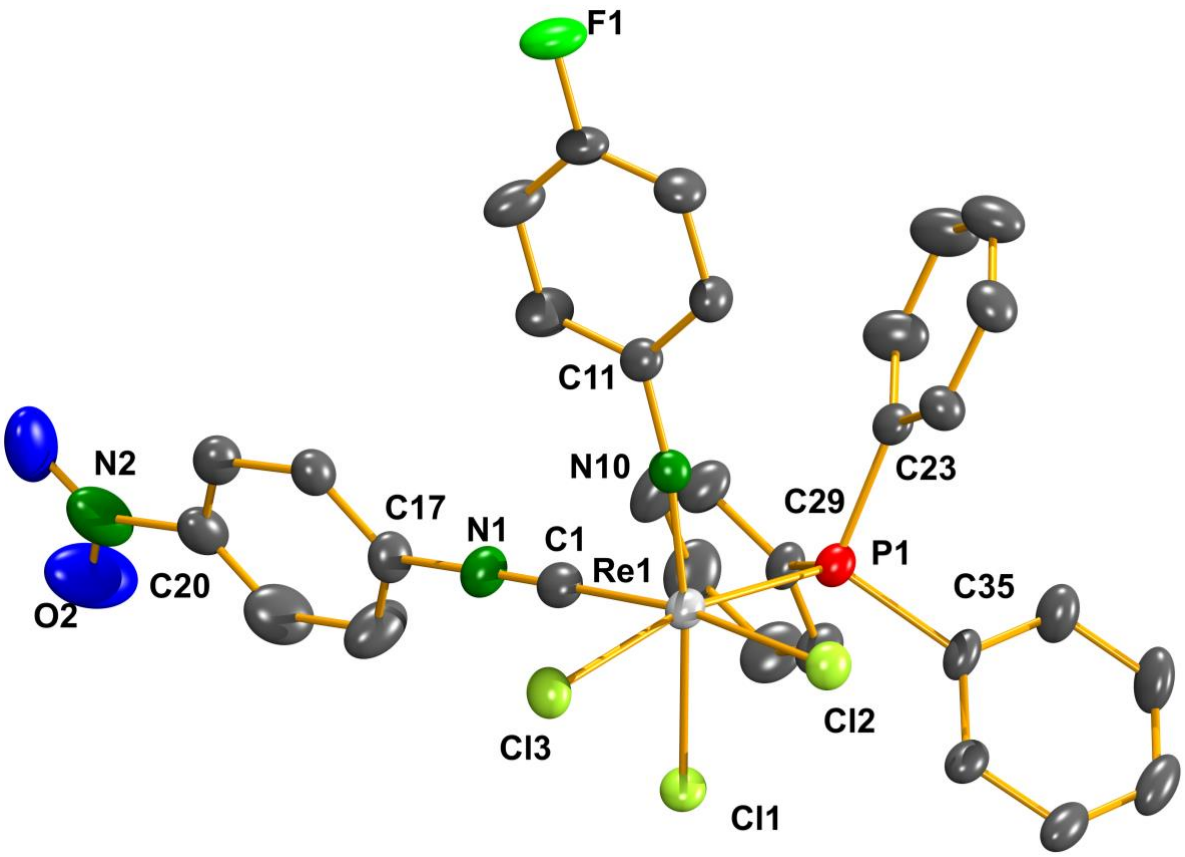

Figure S5: Ellipsoid representation of [Re(NPhF)Cl_3(PPh_3)($CNPh^{pNO2}$)] (**6**). The thermal ellipsoids are set at a 50% probability level. Hydrogen atoms are omitted for clarity.

Table S6: Selected bond lengths (Å) and angles (°) in [Re(NPhF)Cl_3(PPh_3)($CNPh^{pNO2}$)] (**6**).

Re1-Cl2	2.3967(1)	P1-C23	1.827(4)	Re1-Cl3	2.4203(13)
Re1-Cl1	2.4282(1)	P1-C29	1.801(4)	Re1-N10	1.712(3)
Re1-P1	2.4537(1)	P1-C35	1.834(4)	Re1-C1	2.021(5)
N10-C11	1.390(5)	C1-N1	1.162(6)	N1-C17	1.397(6)
Cl2-Re1-Cl1	94.32(4)	Cl1-Re1-P1	82.76(4)	C11-N10-Re1	171.1(3)
Cl2-Re1-P1	88.88(4)	Cl1-Re1-Cl3	86.30(4)	C1-Re1-P1	93.47(14)
Cl2-Re1-Cl3	86.92(4)	Cl3-Re1-P1	167.95(3)	N1-C1-Re1	176.6(4)
C1-Re1-Cl2	171.69(1)	C1-Re1-Cl1	78.09(13)	C1-N1-C17	178.2(5)

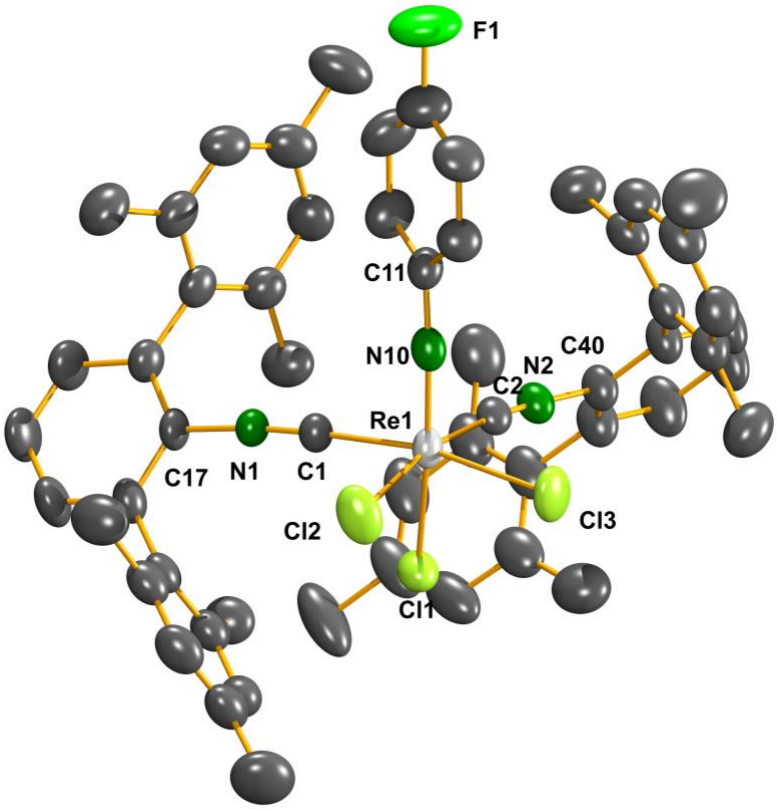

Figure S6: Ellipsoid representation of [Re(NPhF)Cl_3($CNAr^{Mes2}$)$_2$] (**7**). The thermal ellipsoids are set at a 50% probability level. Hydrogen atoms are omitted for clarity.

Table S7: Selected bond lengths (Å) and angles (°) in [Re(NPhF)Cl_3($CNAr^{Mes2}$)$_2$] (**7**)**.**

Re1-Cl2	2.3855(1)	N1-C1	1.140(5)	Re1-Cl3	2.3783(1)
Re1-Cl1	2.4001(1)	N2-C40	1.399(5)	Re1-N10	1.724(3)
C2-N2	1.149(5)	Re1-C2	2.034(4)	Re1-C1	2.043(4)
N10-C11	1.363(5)	N1-C17	1.395(5)	N2-C2	1.149(5)
Cl2-Re1-Cl1	89.12(5)	Cl1-Re1-C2	80.13(1)	C11-N10-Re1	173.0(3)
Cl2-Re1-C2	167.75(1)	Cl2-Re1-Cl3	87.59(5)	C1-Re1-C2	96.89(2)
Cl1-Re1-Cl3	90.24(5)	N2-C2-Re1	174.2(4)	N1-C1-Re1	176.6(3)
C1-Re1-Cl2	86.88(1)	C1-Re1-Cl1	79.77(1)	C1-N1-C17	174.7(4)

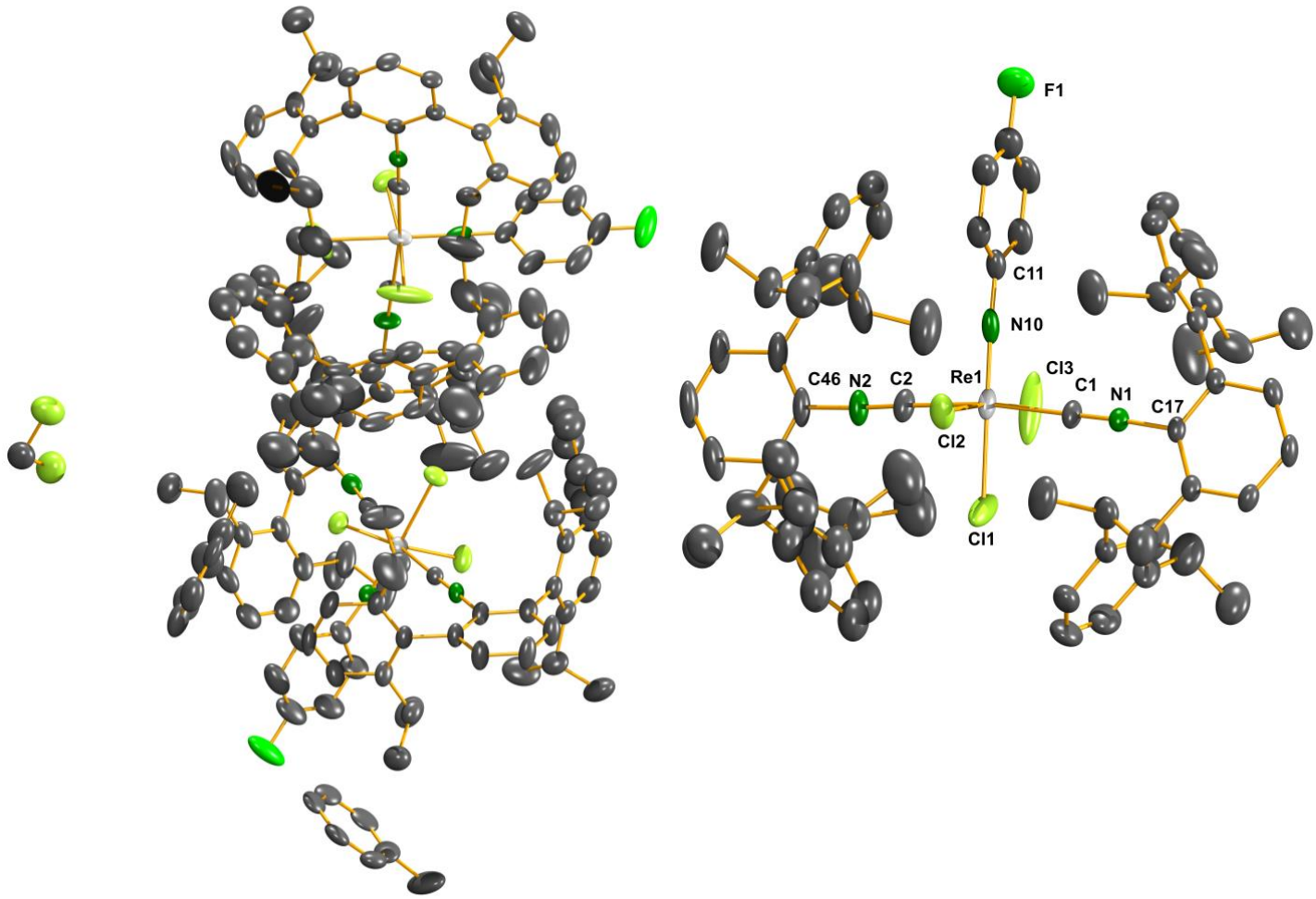

Figure S7A: Ellipsoid representation of $[Re(NPhF)Cl_3(CNAr^{Dipp2})_2]\cdot 1.25$ toluene·1/2 CH_2Cl_2 (**8**), species 1. The thermal ellipsoids are set at a 50% probability level. Hydrogen atoms are omitted for clarity. One of the crystallographically independent species (see labelled compound) shows unusually large ellipsoids for Cl1 and Cl3. This is mainly due to packing effects and have not been constrained by EADP instructions.

Table S8A: Selected bond lengths (Å) and angles (°) in $[Re(NPhF)Cl_3(CNAr^{Dipp2})_2]\cdot 1.25$ toluene·1/2 CH_2Cl_2 (**8**), species 1**.**

Re1-Cl2	2.392(2)	N1-C1	1.142(8)	Re1-Cl3	2.383(2)
Re1-Cl1	2.367(3)	N2-C46	1.412(8)	Re1-N10	1.728(7)
C2-N2	1.155(9)	Re1-C2	2.056(7)	Re1-C1	2.075(6)
N10-C11	1.373(1)	N1-C17	1.394(7)	N2-C2	1.155(9)
Cl2-Re1-Cl1	86.01(12)	Cl1-Re1-C2	86.5(2)	C11-N10-Re1	177.3(5)
Cl2-Re1-C2	91.2(2)	Cl2-Re1-Cl3	173.66(2)	C1-Re1-C2	172.3(3)
Cl1-Re1-Cl3	87.68(2)	N2-C2-Re1	176.5(7)	N1-C1-Re1	179.0(7)
C1-Re1-Cl2	90.29(19)	C1-Re1-Cl1	86.0(2)	C1-N1-C17	176.8(6)

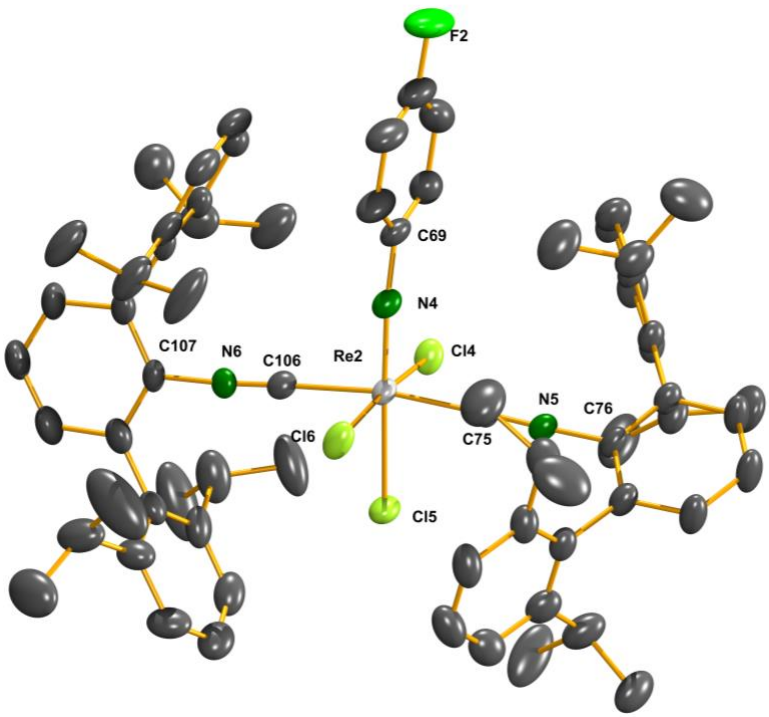

Figure S7B: Ellipsoid representation of $[Re(NPhF)Cl_3(CNAr^{Dipp2})_2]$ 1.25 toluene·1/2 CH_2Cl_2 (**8**), species 2. The thermal ellipsoids are set at a 50% probability level. Hydrogen atoms are omitted for clarity.

Table S8B: Selected bond lengths (Å) and angles (°) in $[Re(NPhF)Cl_3(CNAr^{Dipp2})_2]$ ·1.25 toluene·1/2 CH_2Cl_2 (**8**), species 2**.**

Re2-Cl4	2.4267(2)	N5-C76	1.145(8)	Re2-Cl6	2.3975(2)
Re2-Cl5	2.3801(2)	N6-C106	1.415(8)	Re2-N4	1.722(6)
C106-N6	1.160(9)	Re2-C106	2.055(7)	Re2-C75	2.066(6)
N6-C107	1.409(9)	N4-C69	1.370(9)	N5-C75	1.151(8)
C75-Re2-Cl5	85.66(2)	Cl4-Re2-C106	94.1(3)	C69-N4-Re2	171.5(6)
Cl5-Re2-C106	86.0(2)	Cl5-Re2-Cl6	87.54(7)	C106-Re2-C75	171.6(3)
Cl4-Re2-Cl6	172.88(7)	N6-C106-Re2	178.3(6)	N5-C75-Re2	178.2(6)
C75-Re2-Cl5	85.66(2)	C106-Re2-Cl4	89.63(2)	C75-N5-C76	177.5(&)

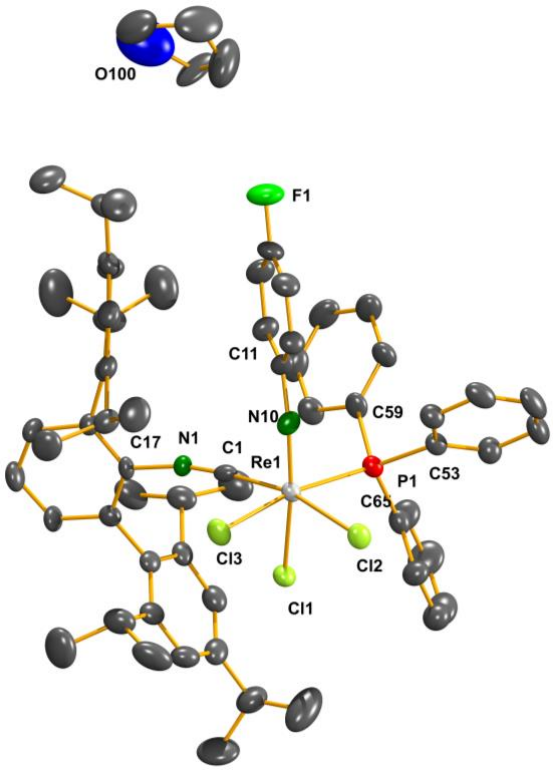

Figure S8: Ellipsoid representation of [Re(NPhF)Cl_3(PPh_3)($CNAr^{Tripp2}$)]·THF (**9**). The thermal ellipsoids are set at a 50% probability level. Hydrogen atoms are omitted for clarity.

Table S9: Selected bond lengths (Å) and angles (°) in [Re(NPhF)Cl_3(PPh_3)($CNAr^{Tripp2}$)]·THF (**9**).

Re1-Cl2	2.3958(1)	P1-C53	1.824(5)	Re1-Cl3	2.4173(2)
Re1-Cl1	2.3771(2)	P1-C59	1.823(5)	Re1-N10	1.711(4)
Re1-P1	2.4602 (2)	P1-C65	1.805(5)	Re1-C1	2.027(5)
N10-C11	1.409(6)	C1-N1	1.167(5)	N1-C17	1.405(5)
Cl2-Re1-Cl1	86.17(5)	Cl1-Re1-P1	86.23(5)	C11-N10-Re1	168.7(3)
Cl2-Re1-P1	86.17(5)	Cl1-Re1-Cl3	87.59(5)	C1-Re1-P1	100.96(14)
Cl2-Re1-Cl3	86.56(5)	Cl3-Re1-P1	170.35(5)	N1-C1-Re1	170.4(4)
C1-Re1-Cl2	166.31(14)	C1-Re1-Cl1	77.82(14)	C1-N1-C17	164.9(5)

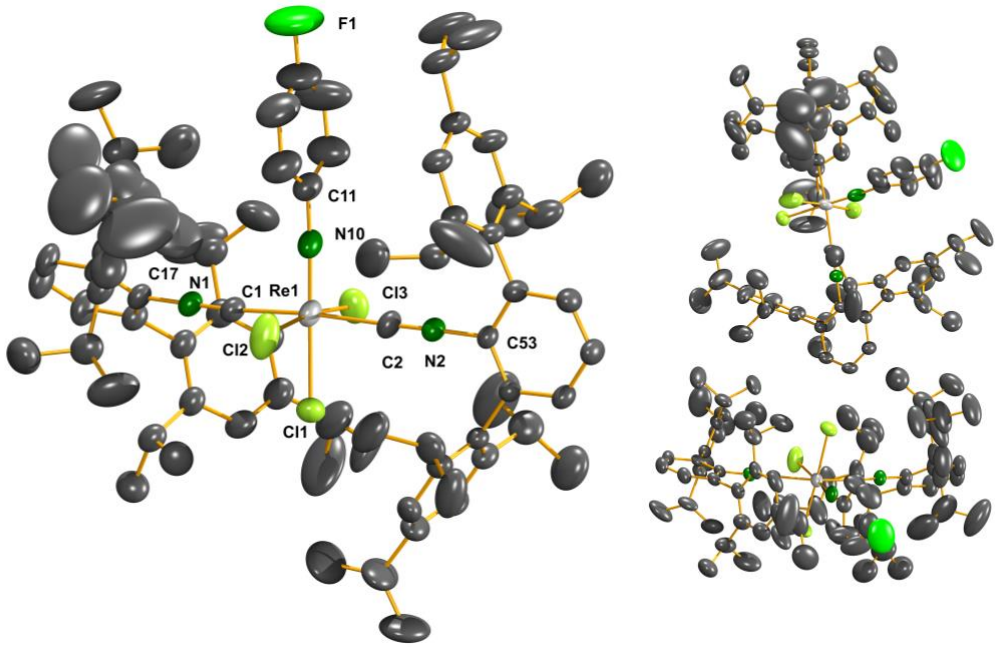

Figure S9A: Ellipsoid representation of [Re(NPhF)Cl_3($CNAr^{Tripp2}$)$_2$] (**10**), species 1. The thermal ellipsoids are set at a 50% probability level. Hydrogen atoms are omitted for clarity.

Table S10A: Selected bond lengths (Å) and angles (°) in [Re(NPhF)Cl_3($CNAr^{Tripp2}$)$_2$] (**10**), species 1**.**

Re1-Cl2	2.417(2)	N1-C1	1.135(7)	Re1-Cl3	2.3972(2)
Re1-Cl1	2.3627(2)	N2-C53	1.412(6)	Re1-N10	1.698(6)
C2-N2	1.139(7)	Re1-C2	2.084(6)	Re1-C1	2.093(6)
N10-C11	1.397(8)	N1-C17	1.408(7)		
Cl2-Re1-Cl1	85.81(8)	Cl1-Re1-C2	86.25(2)	C11-N10-Re1	177.1(5)
Cl2-Re1-C2	93.07(2)	Cl2-Re1-Cl3	171.09(9)	C1-Re1-C2	173.9(2)
Cl1-Re1-Cl3	85.32(7)	N2-C2-Re1	177.3(6)	N1-C1-Re1	177.3(6)
C1-Re1-Cl2	89.32(19)	C1-Re1-Cl1	88.38(2)	C1-N1-C17	178.4(7)

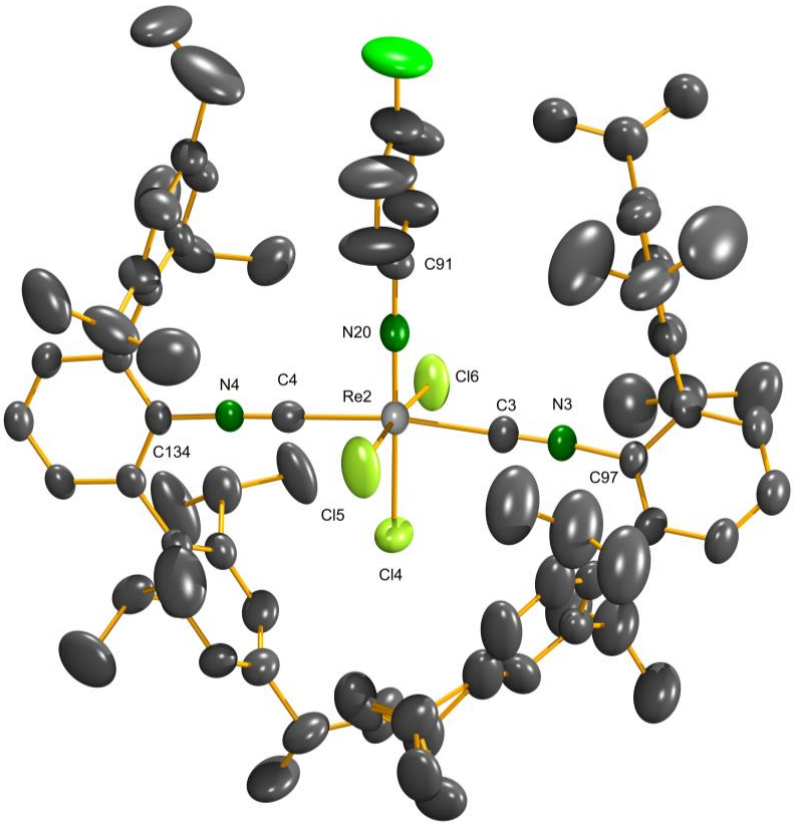

Figure S9B: Ellipsoid representation of [Re(NPhF)Cl_3($CNAr^{Tripp2}$)$_2$] (**10**), species 2. The thermal ellipsoids are set at a 50% probability level. Hydrogen atoms are omitted for clarity.

Table S10B: Selected bond lengths (Å) and angles (°) in [Re(NPhF)Cl_3($CNAr^{Tripp2}$)$_2$] (**10**), species 2**.**

Re2-Cl5	2.4016(2)	N3-C3	1.135(7)	Re2-Cl6	2.4016(2)
Re2-Cl4	2.3609(2)	N3-C97	1.397(7)	Re2-N20	1.711(5)
C4-N4	1.148(7)	Re2-C4	2.076(6)	Re2-C3	2.090(6)
N20-C91	1.376(8)	N3-C97	1.397(7)		
C4-Re2-Cl4	84.67(2)	Cl4-Re2-C4	84.67(2)	C91-N20-Re2	178.7(5)
Cl5-Re2-C4	88.52(2)	Cl5-Re2-Cl6	173.17(9)	C3-Re2-C4	170.8(2)
Cl4-Re2-Cl6	86.17(9)	N4-C4-Re2	179.5(7)	N3-C3-Re2	175.4(5)
C3-Re2-Cl5	92.44(2)	C3-Re2-Cl4	86.23(2)	C4-N4-C134	177.2(6)

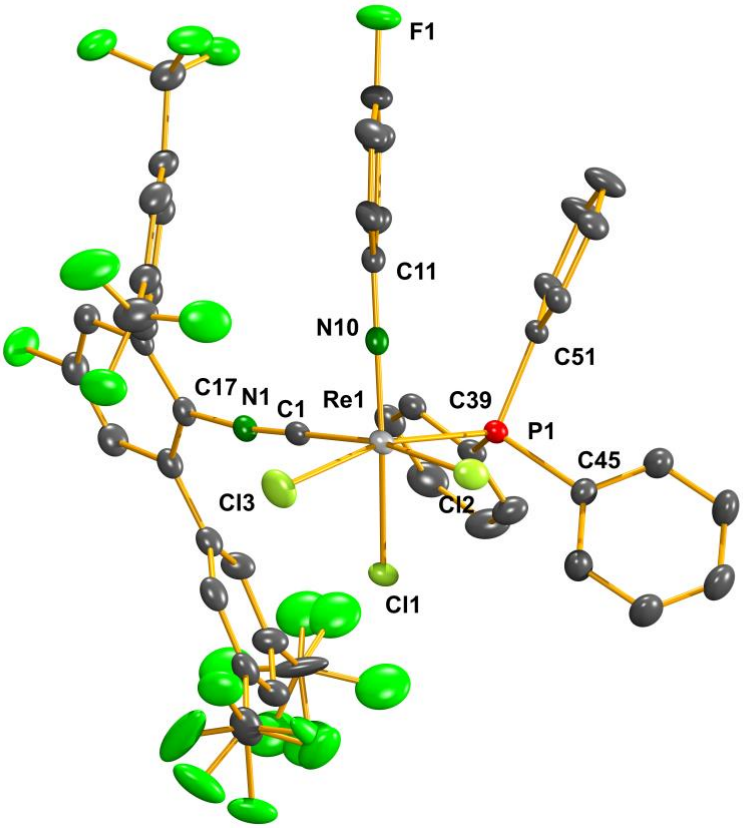

Figure S10: Ellipsoid representation of [Re(NPhF)Cl_3(PPh_3)(CNp-FAr^{DarF2})] (**11**). The thermal ellipsoids are set at a 50% probability level. Hydrogen atoms are omitted for clarity.

Table S11: Selected bond lengths (Å) and angles (°) in [Re(NPhF)Cl_3(PPh_3)(CNp-FAr^{DarF2})] (**11**).

Re1-Cl2	2.4013(8)	P1-C39	1.816(3)	Re1-Cl3	2.3879(8)
Re1-Cl1	2.4253(7)	P1-C45	1.835(3)	Re1-N10	1.721(3)
Re1-P1	2.4494(8)	P1-C51	1.822(3)	Re1-C1	2.022(3)
N10-C11	1.380(4)	C1-N1	1.151(4)	N1-C17	1.393(4)
Cl2-Re1-Cl1	94.67(3)	Cl1-Re1-P1	79.30(3)	C11-N10-Re1	170.4(2)
Cl2-Re1-P1	89.00(3)	Cl1-Re1-Cl3	86.86(3)	C1-Re1-P1	96.37(8)
Cl2-Re1-Cl3	86.10(3)	Cl3-Re1-P1	164.88(3)	N1-C1-Re1	174.6(3)
C1-Re1-Cl2	169.98(9)	C1-Re1-Cl1	78.10(8)	C1-N1-C17	172.2(3)

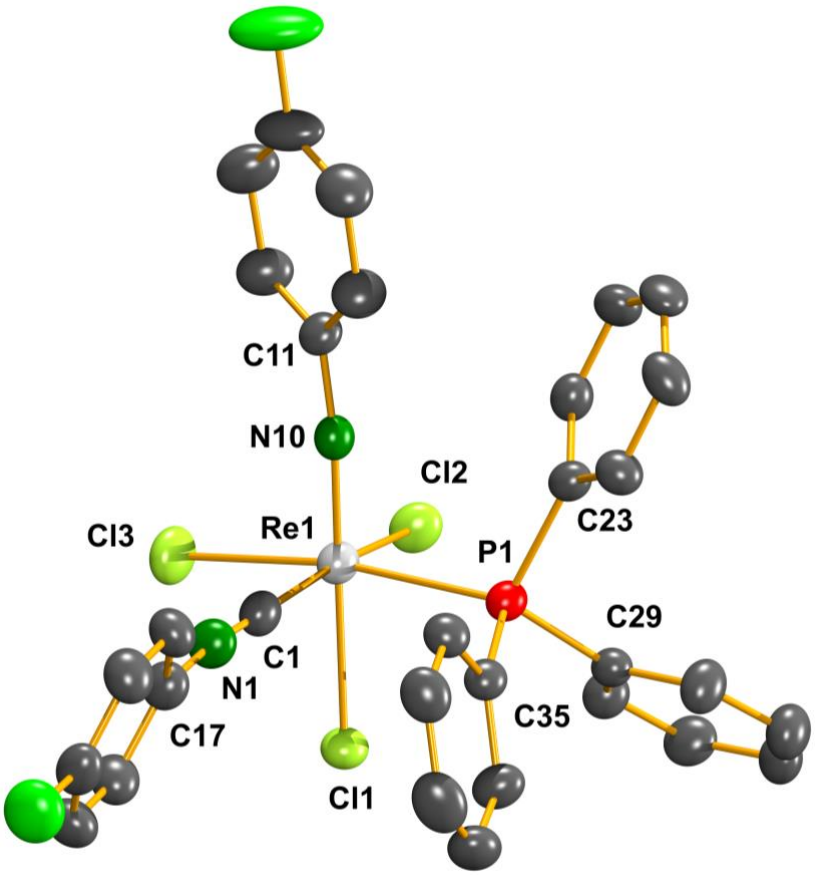

Figure S11: Ellipsoid representation of [Re(NPhF)Cl_3(PPh3)(CNPh^{pF})] (**12**). The thermal ellipsoids are set at a 50% probability level. Hydrogen atoms are omitted for clarity.

Table S12: Selected bond lengths (Å) and angles (°) in [Re(NPhF)Cl_3(PPh3)(CNPh^{pF})] (**12**).

Re1-Cl2	2.407(2)	P1-C23	1.832(5)	Re1-Cl3	2.4129(2)
Re1-Cl1	2.437(2)	P1-C35	1.822(5)	Re1-N10	1.705(4)
Re1-P1	2.470(2)	P1-C29	1.833(5)	Re1-C1	2.024(6)
N10-C11	1.395(7)	C1-N1	1.156(7)	N1-C17	1.396(7)
Cl2-Re1-Cl1	89.91(5)	Cl1-Re1-P1	81.81(5)	C11-N10-Re1	172.9(4)
Cl2-Re1-P1	93.14(5)	Cl1-Re1-Cl3	88.81(6)	C1-Re1-P1	91.33(16)
Cl2-Re1-Cl3	86.95(6)	Cl3-Re1-P1	170.62(5)	N1-C1-Re1	176.9(5)
C1-Re1-Cl2	169.89(16)	C1-Re1-Cl1	81.75(16)	C1-N1-C17	173.0(6)

Spectroscopic data and mass spectrometry

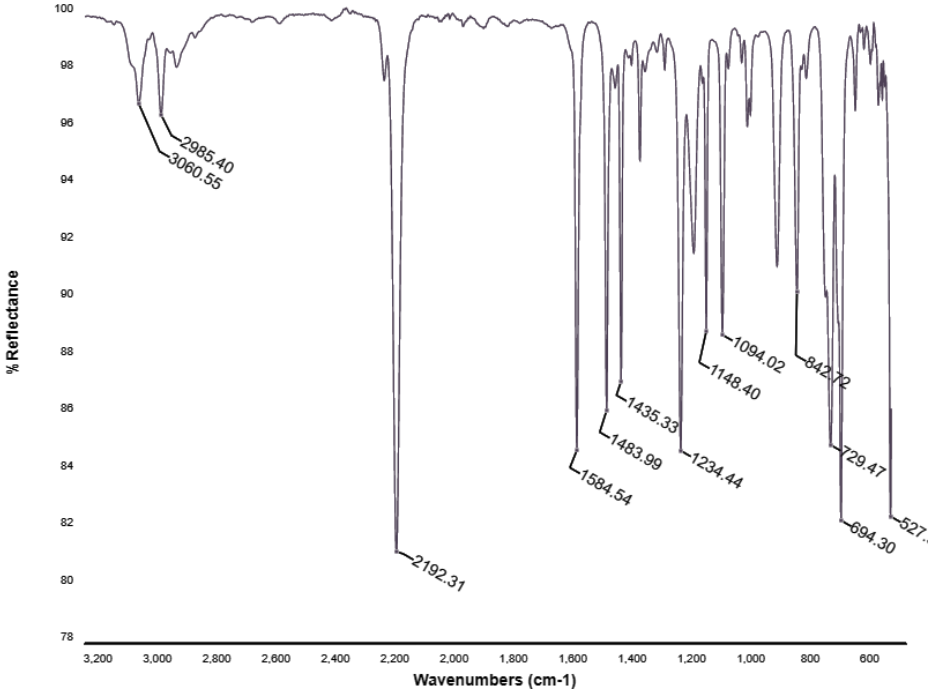

Figure S12: IR (ATR) spectrum of [Re(NPhF)Cl_3(PPh_3)(CN^{t}Bu)] (**2**).

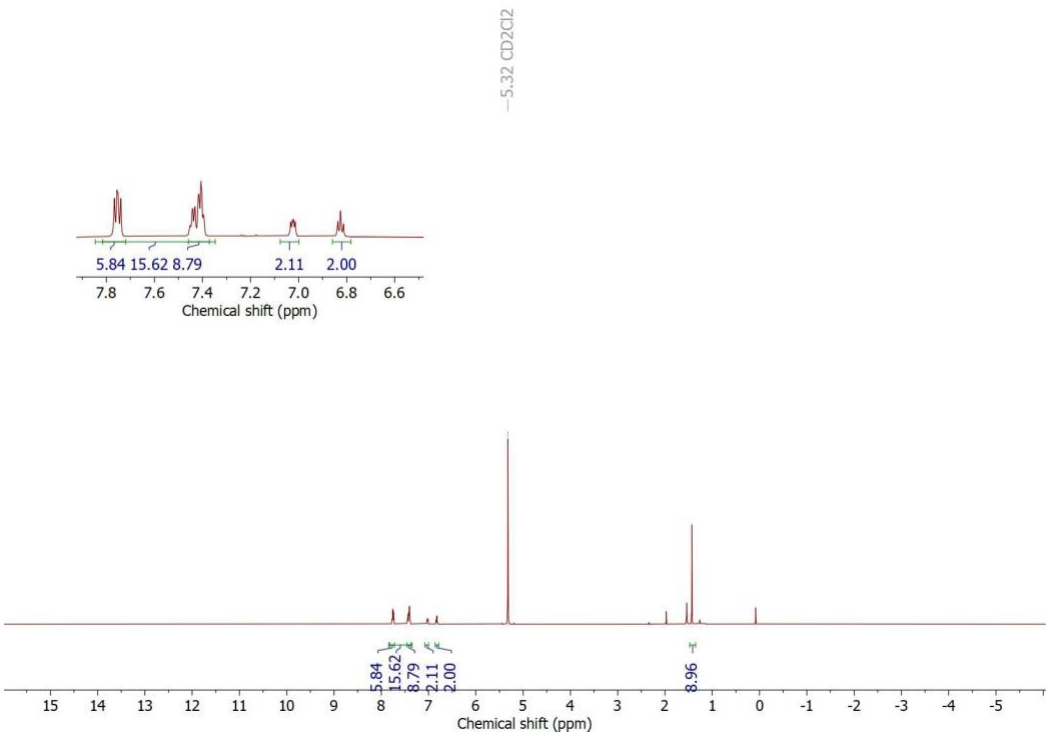

Figure S13: ^{1}H NMR spectrum of [Re(NPhF)Cl_3(PPh_3)(CN^{t}Bu)] (**2**) in CD_2Cl_2.

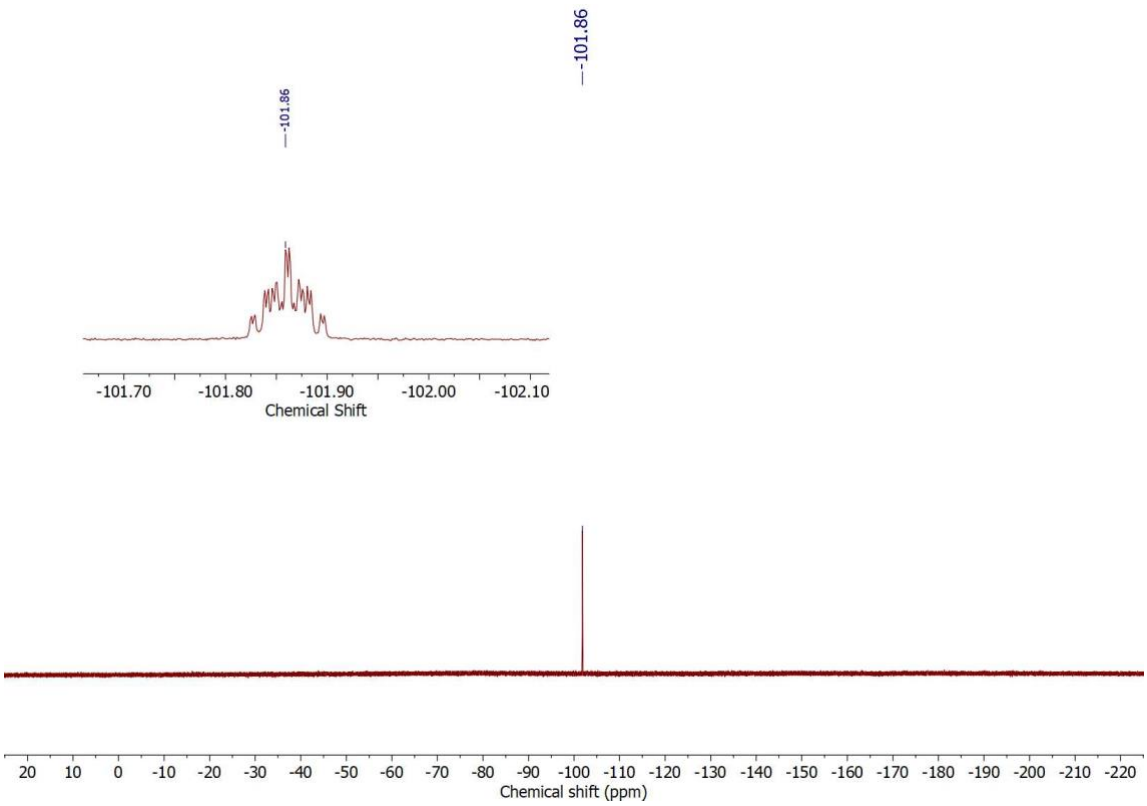

Figure S14: ^{19}F NMR spectrum of [Re(NPhF)Cl_3(PPh_3)(CN^{t}Bu)] (**2**) in CD_2Cl_2.

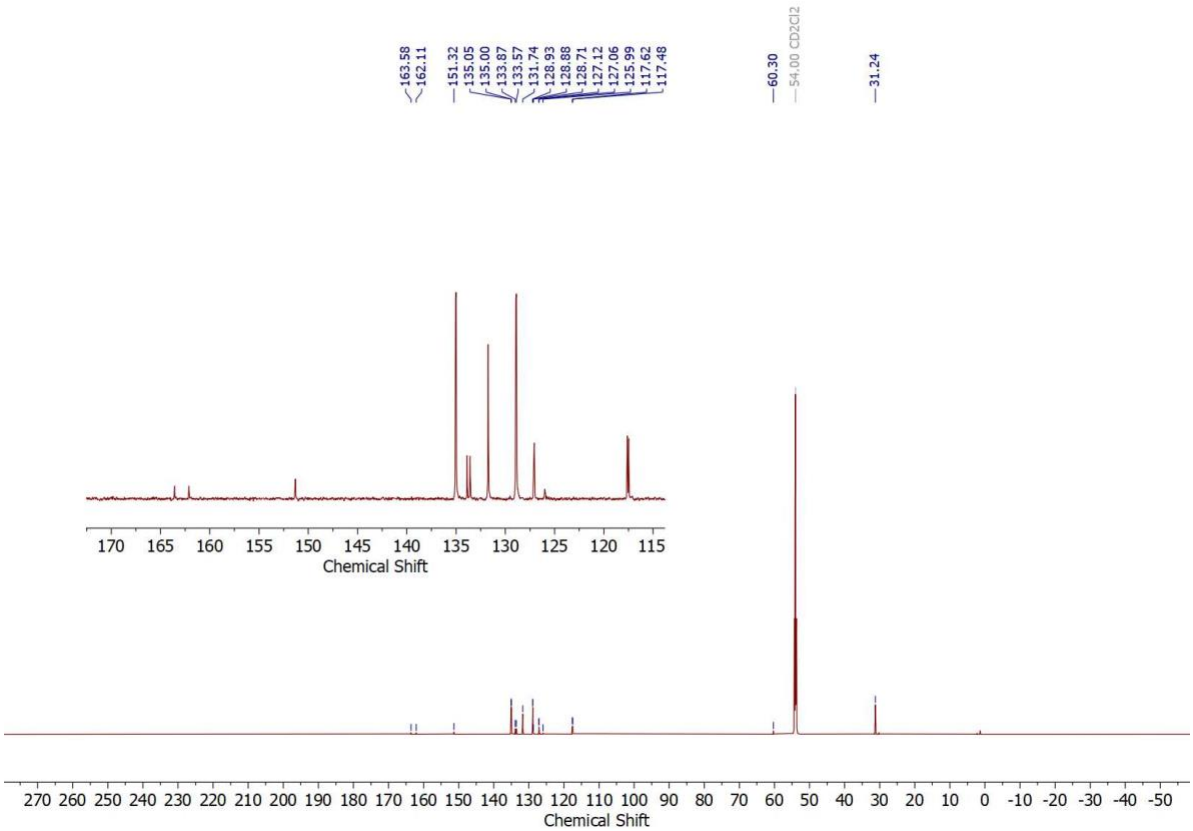

Figure S15: ^{13}C{^{1}H} NMR spectrum of [Re(NPhF)Cl_3(PPh_3)(CN^{t}Bu)] (**2**) in CD_2Cl_2.

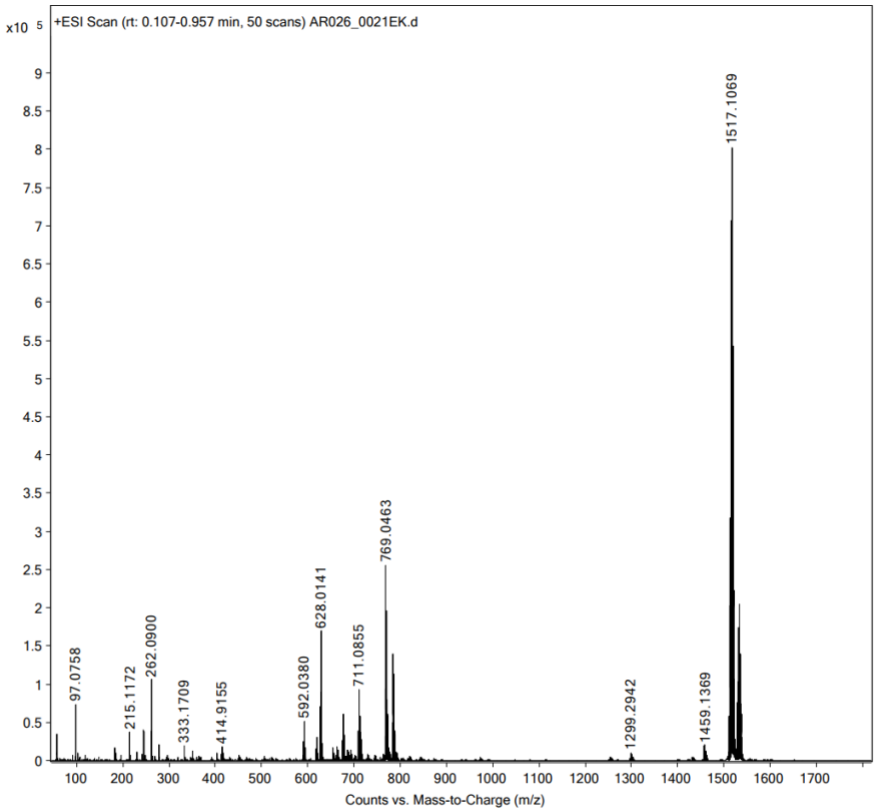

Figure S16: ESI+ mass spectrum of [Re(NPhF)Cl_3(PPh_3)(CN^{t}Bu)] (**2**) in MeCN.

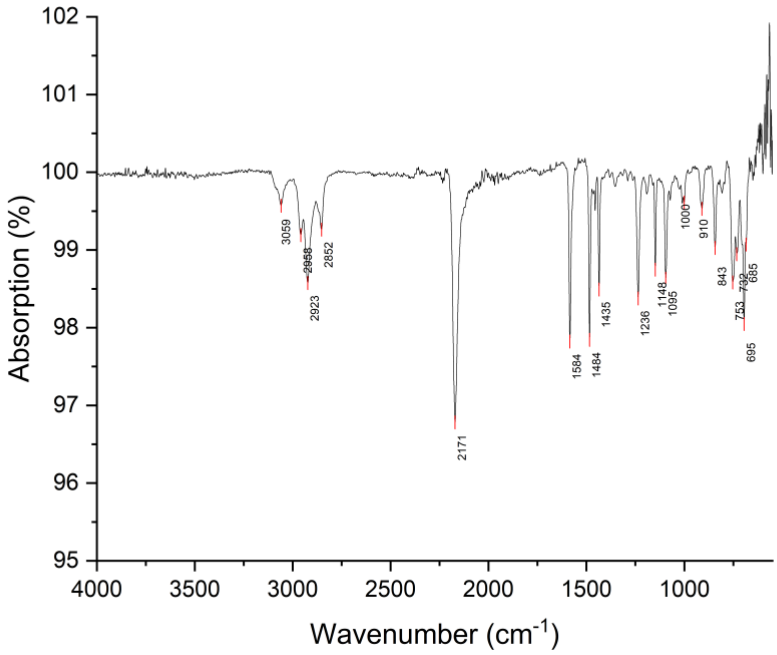

Figure S17: IR (ATR) spectrum of [Re(NPhF)Cl_3(PPh_3)(CNPh)] (**3**).

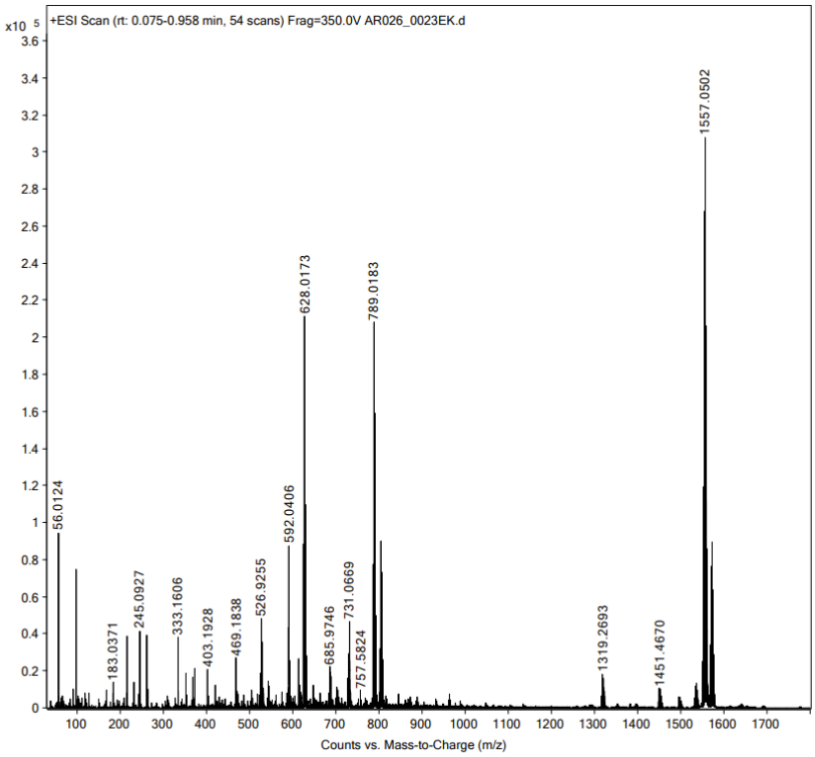

Figure S18: ESI+ mass spectrum of [Re(NPhF)Cl_3(PPh_3)(CNPh)] (**3**) in MeCN.

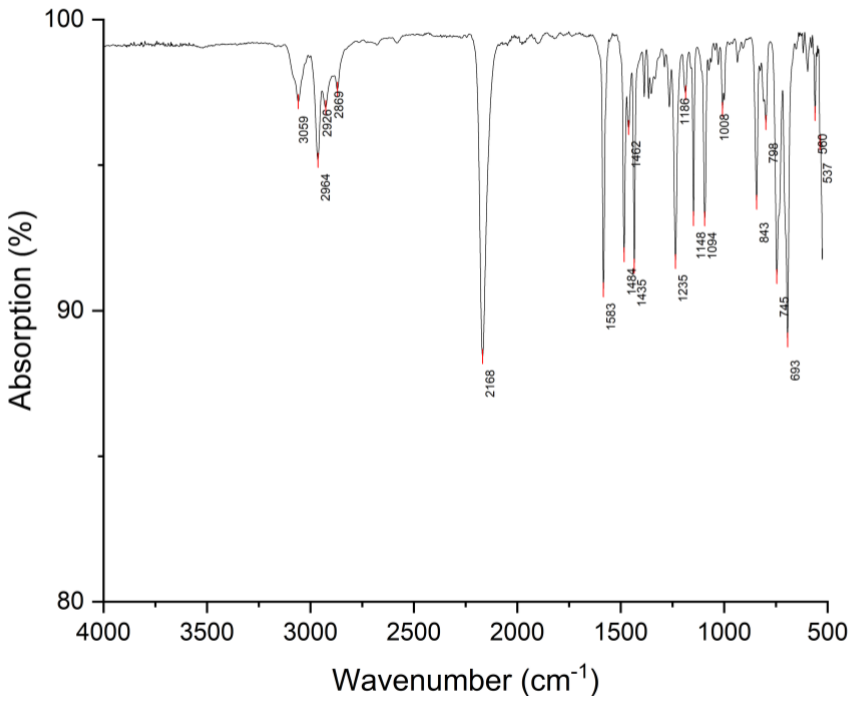

Figure S19: IR (ATR) spectrum of [Re(NPhF)Cl_3(PPh_3)($CNPh^{i\text{-}prop2}$)] (**3**).

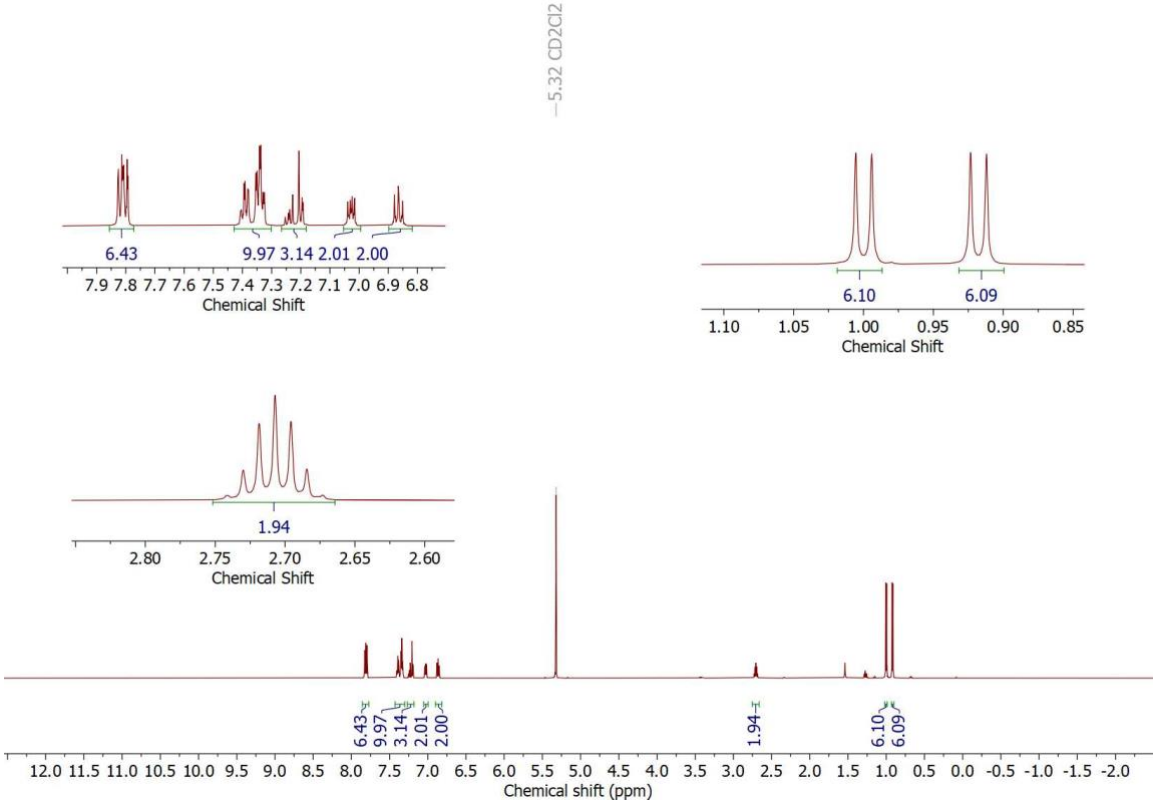

Figure S20: ^{1}H NMR spectrum of [Re(NPhF)Cl_3(PPh_3)(CNPh$^{i\text{-prop2}}$)] (**4**) in CD_2Cl_2.

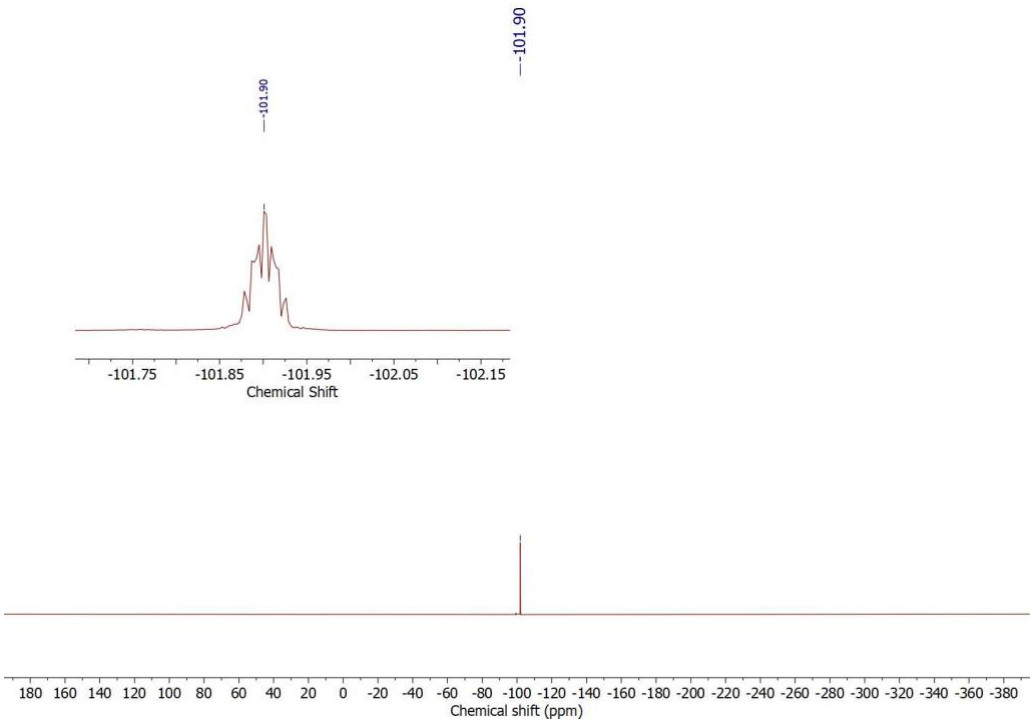

Figure S21: ^{19}F NMR spectrum of [Re(NPhF)Cl_3(PPh_3)(CNPh$^{i\text{-prop2}}$)] (**4**) in CD_2Cl_2.

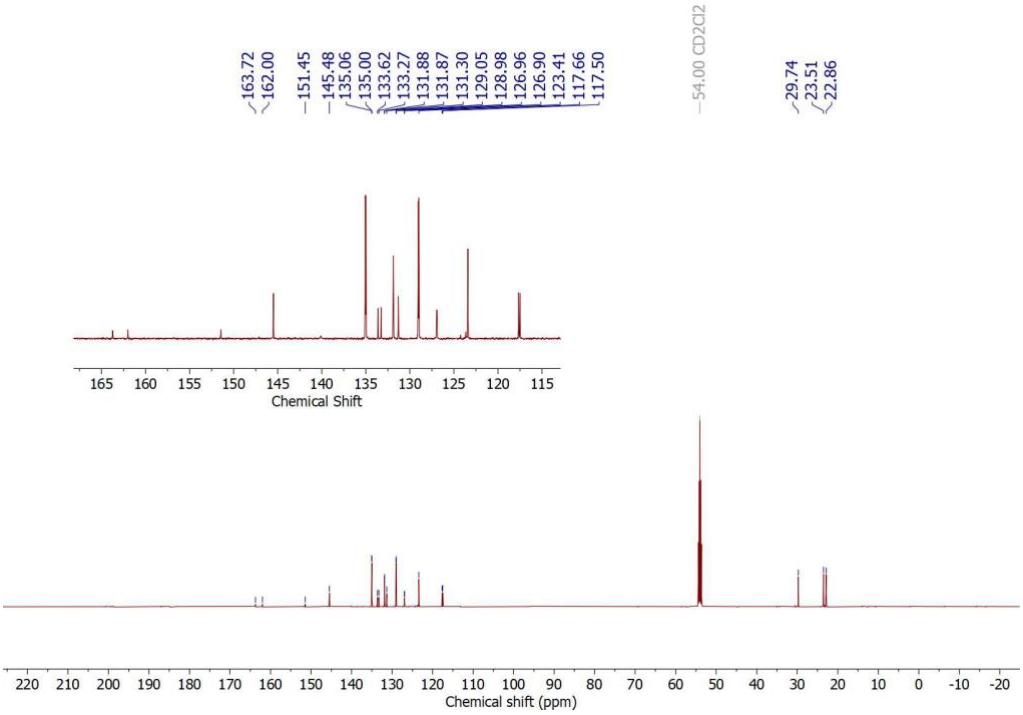

Figure S22: $^{13}C\{^{1}H\}$ NMR of $[Re(NPhF)Cl_3(PPh_3)(CNPh^{i\text{-}prop2})]$ (**4**) in CD_2Cl_2.

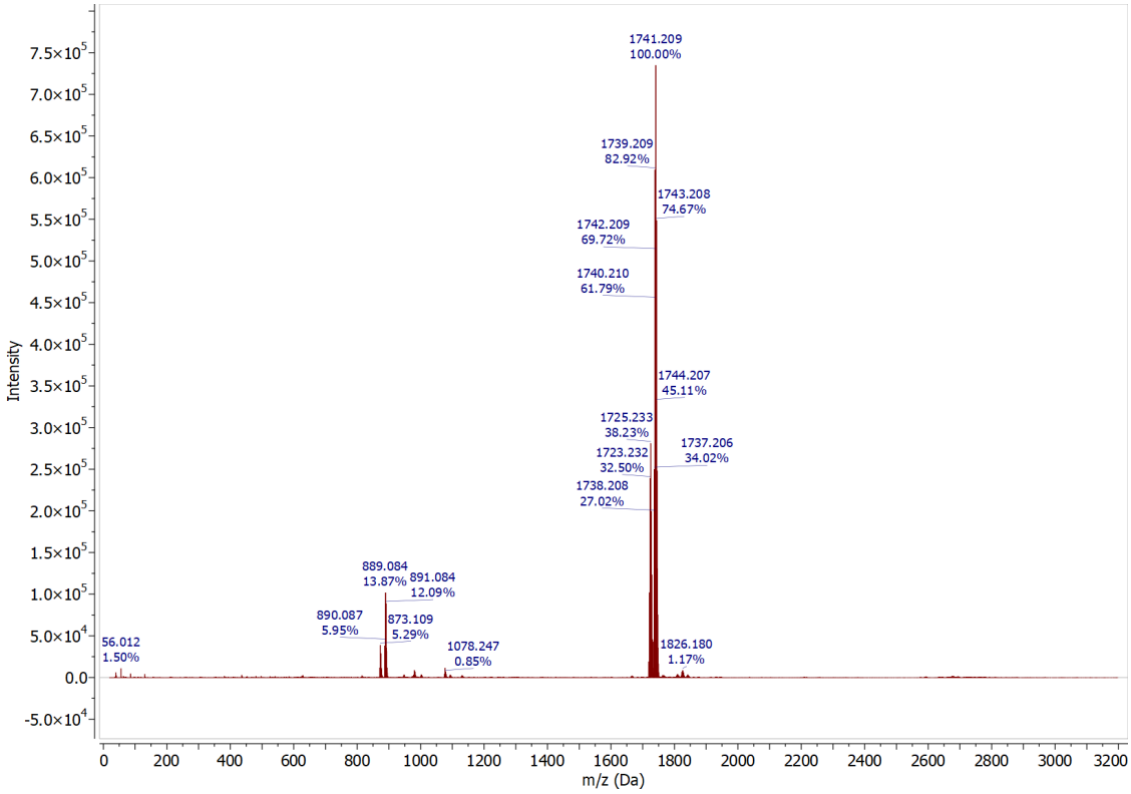

Figure S23: ESI+ mass spectrum of $[Re(NPhF)Cl_3(PPh_3)(CNPh^{i\text{-}prop2})]$ (**4**) in MeCN.

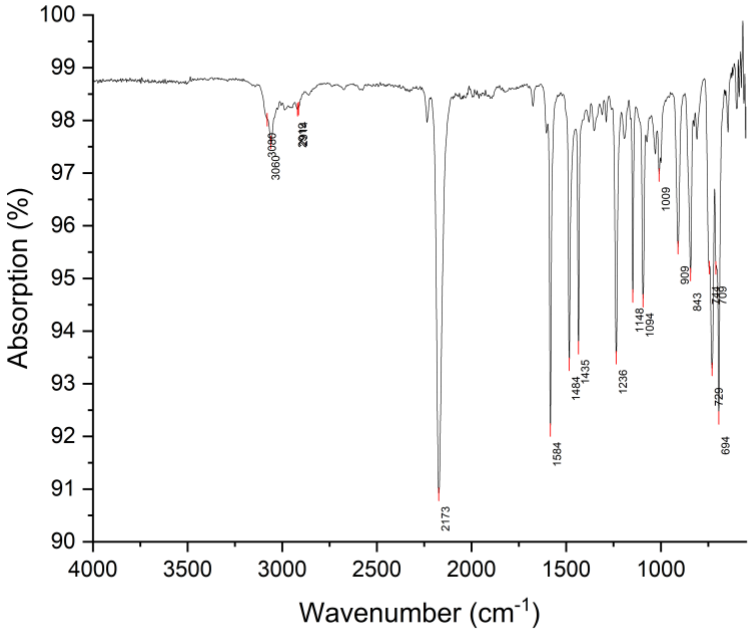

Figure S24: IR (ATR) spectrum of [Re(NPhF)Cl_3(PPh_3)(CNMes)] (**5**).

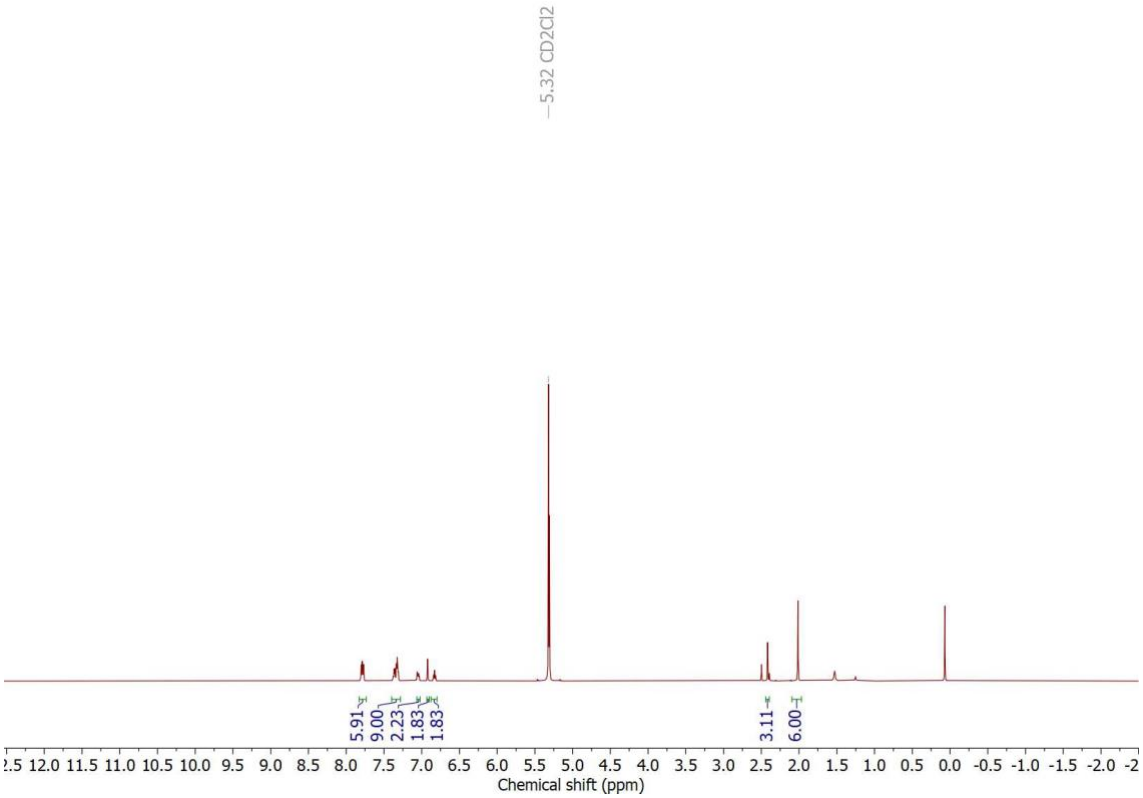

Figure S25: ^{1}H NMR spectrum of [Re(NPhF)Cl_3(PPh_3)(CNMes)] (**5**) in CD_2Cl_2 shortly after dissolution.

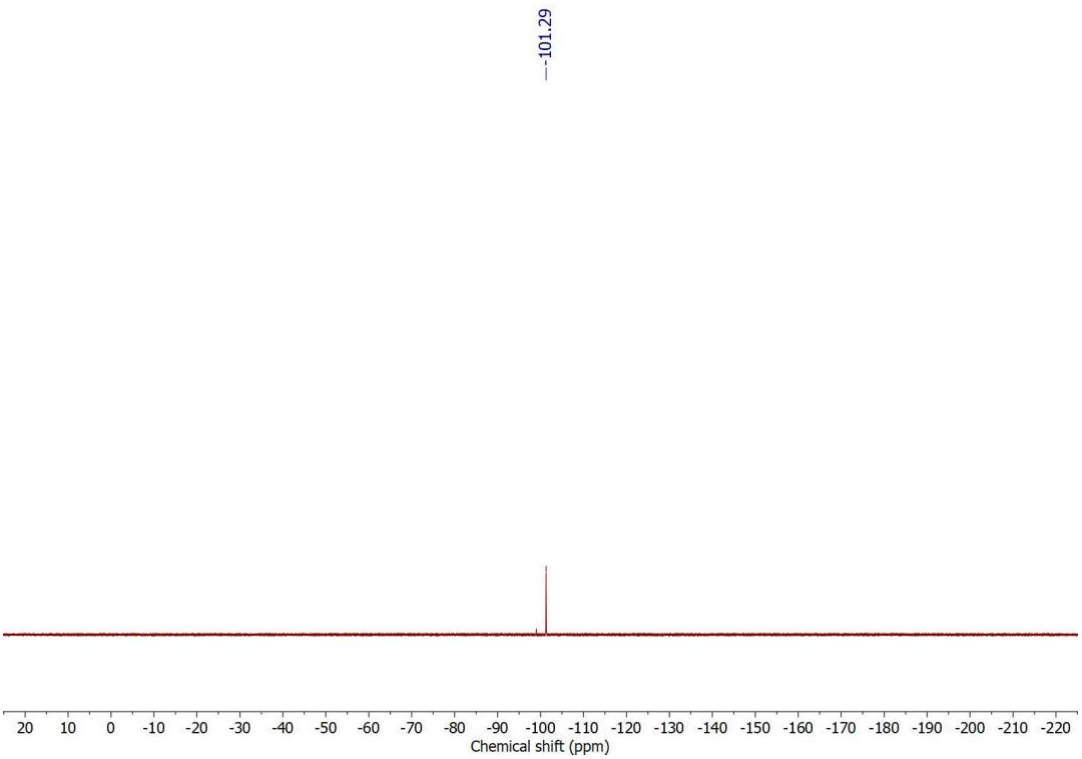

Figure S26: ^{19}F NMR spectrum of [Re(NPhF)Cl_3(PPh_3)(CNMes)] (**5**) in CD_2Cl_2 shortly after dissolution.

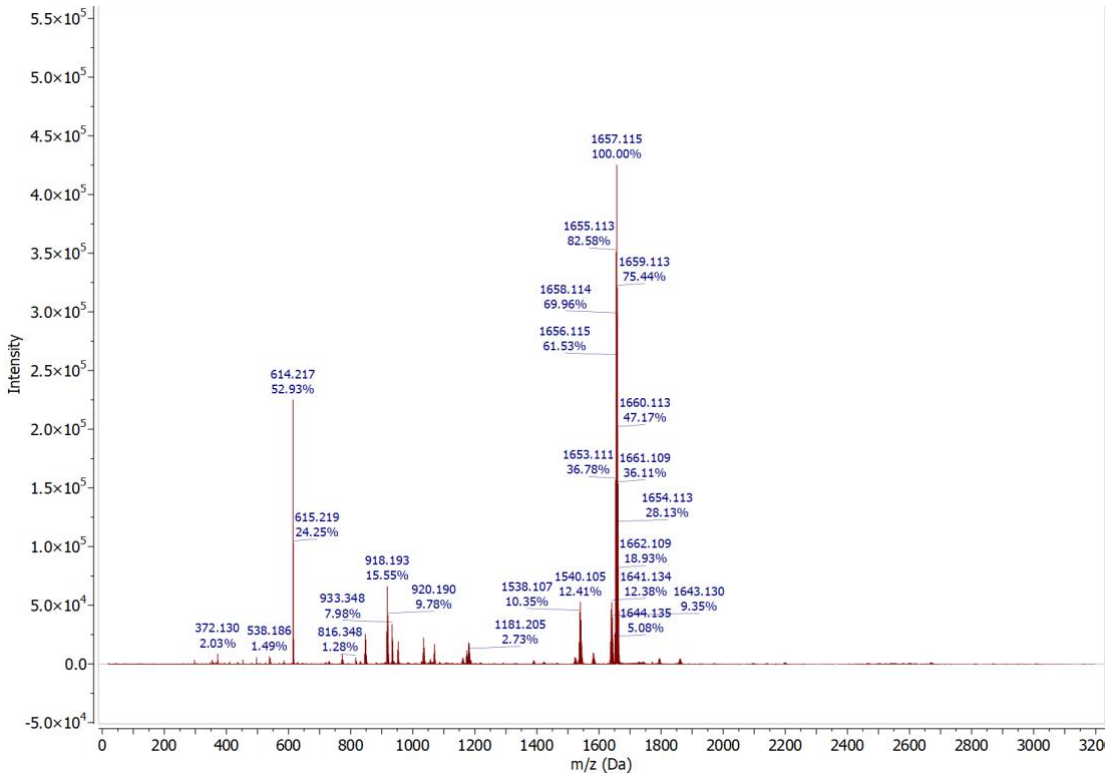

Figure S27: ESI+ mass spectrum of [Re(NPhF)Cl_3(PPh_3)(CNMes)] (**5**) in MeCN.

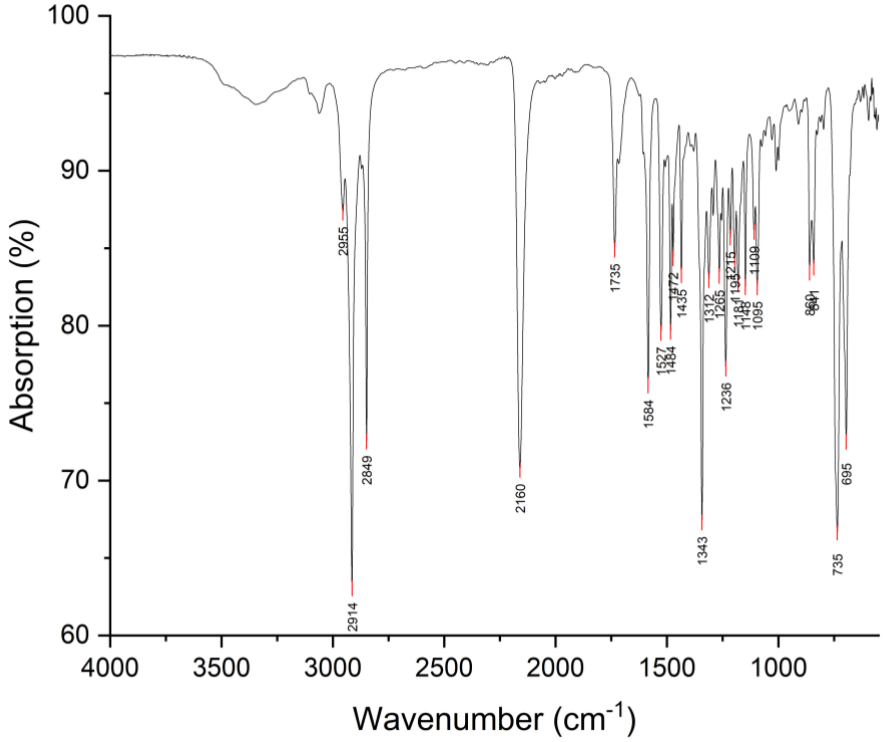

Figure S28: IR (ATR) spectrum of [Re(NPhF)Cl_3(PPh_3)(CNPh^{pNO2})] (**6**).

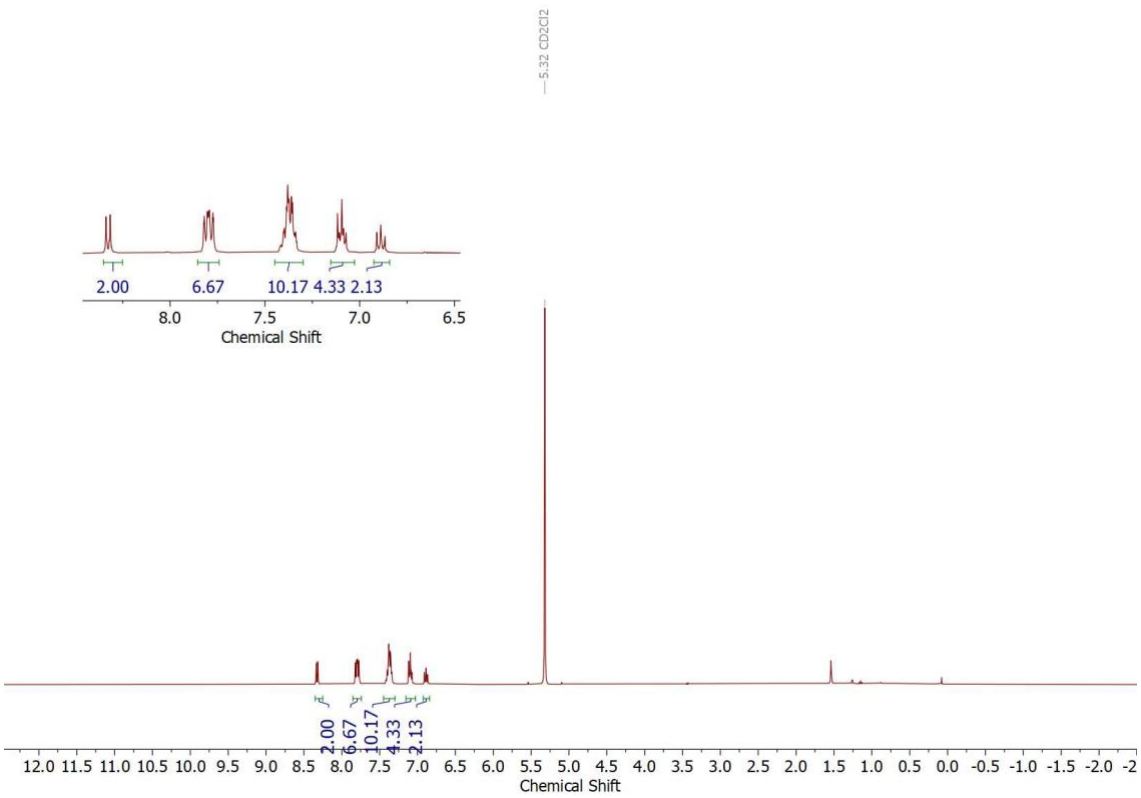

Figure S29: ^{1}H NMR spectrum of [Re(NPhF)Cl_3(PPh_3)(CNPh^{pNO2})] (**6**) in CD_2Cl_2 shortly after dissolution.

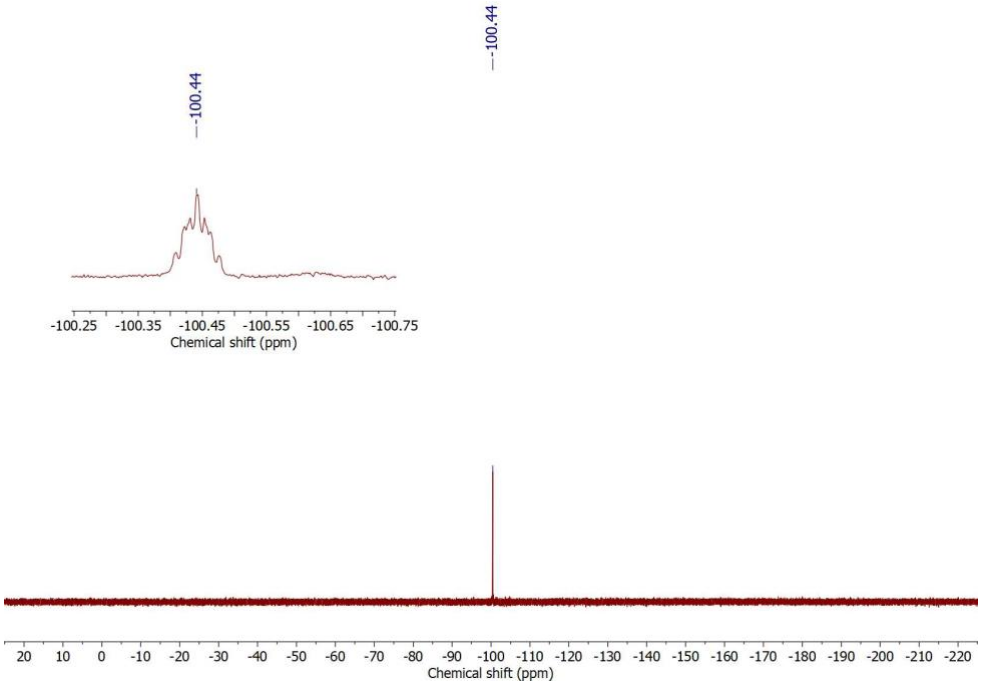

Figure S30: ^{19}F NMR spectrum of [Re(NPhF)Cl_3(PPh_3)(CNPh^{pNO2})] (**6**) in CD_2Cl_2 shortly after dissolution.

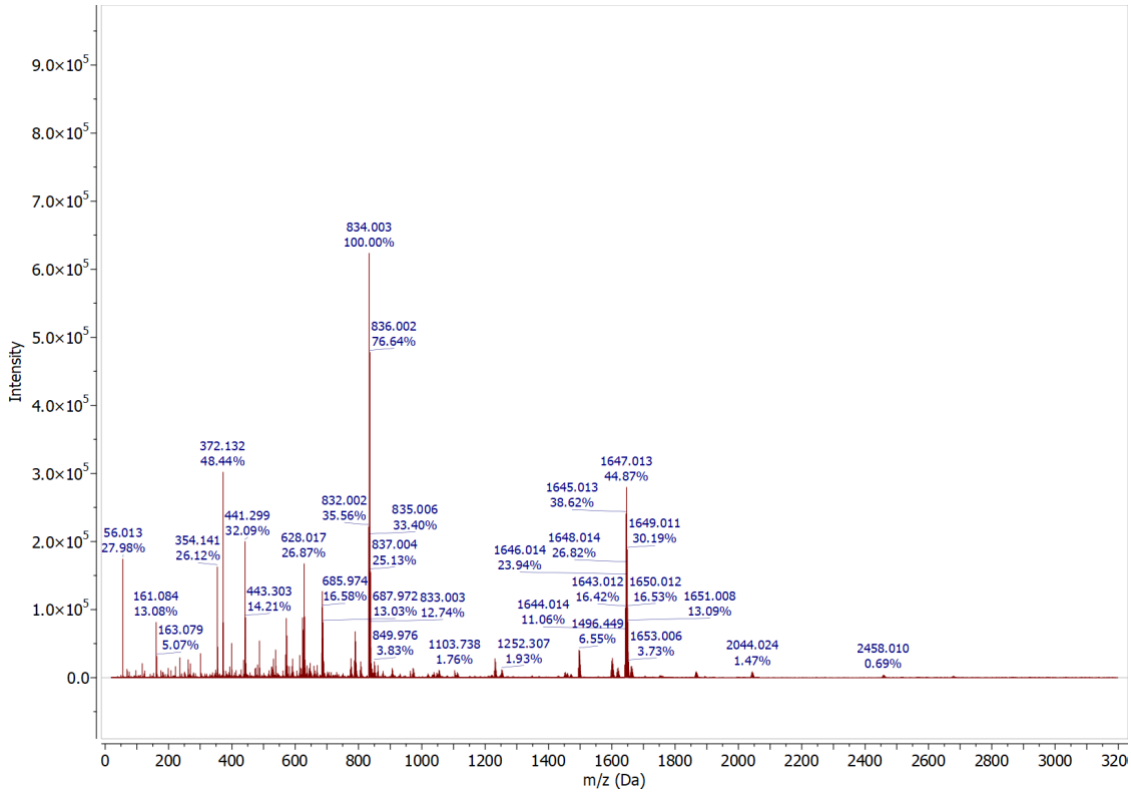

Figure S31: ESI+ mass spectrum of [Re(NPhF)Cl_3(PPh_3)(CNPh^{pNO2})] (**6**) in MeCN.

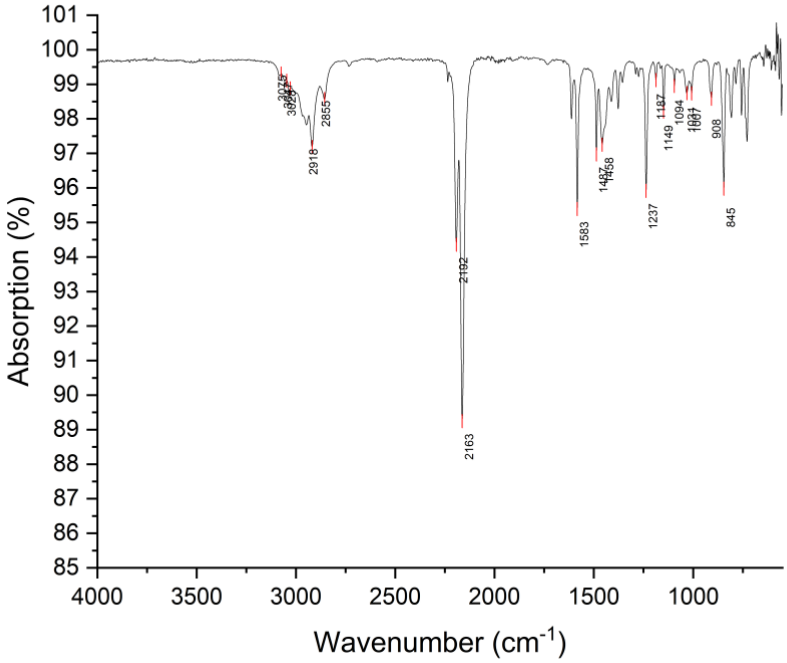

Figure S32: IR (ATR) spectrum of [Re(NPhF)Cl_3($CNAr^{Mes2}$)$_2$] (**7**).

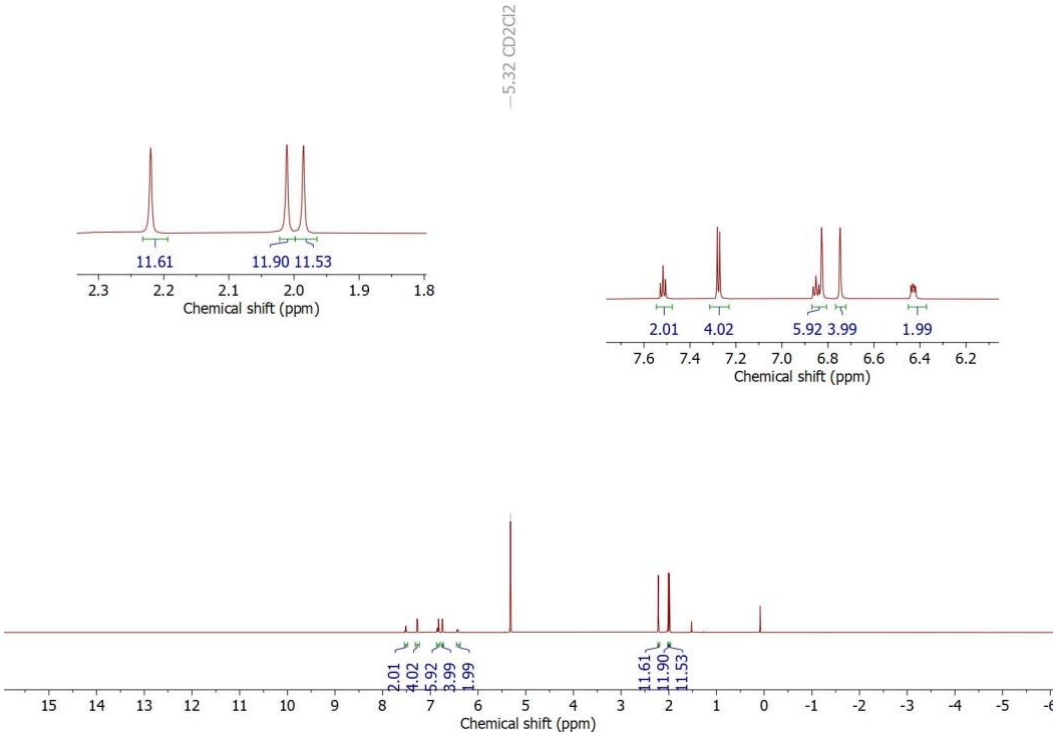

Figure S33: ^{1}H NMR spectrum of [Re(NPhF)Cl_3($CNAr^{Mes2}$)$_2$] (**7**) in CD_2Cl_2.

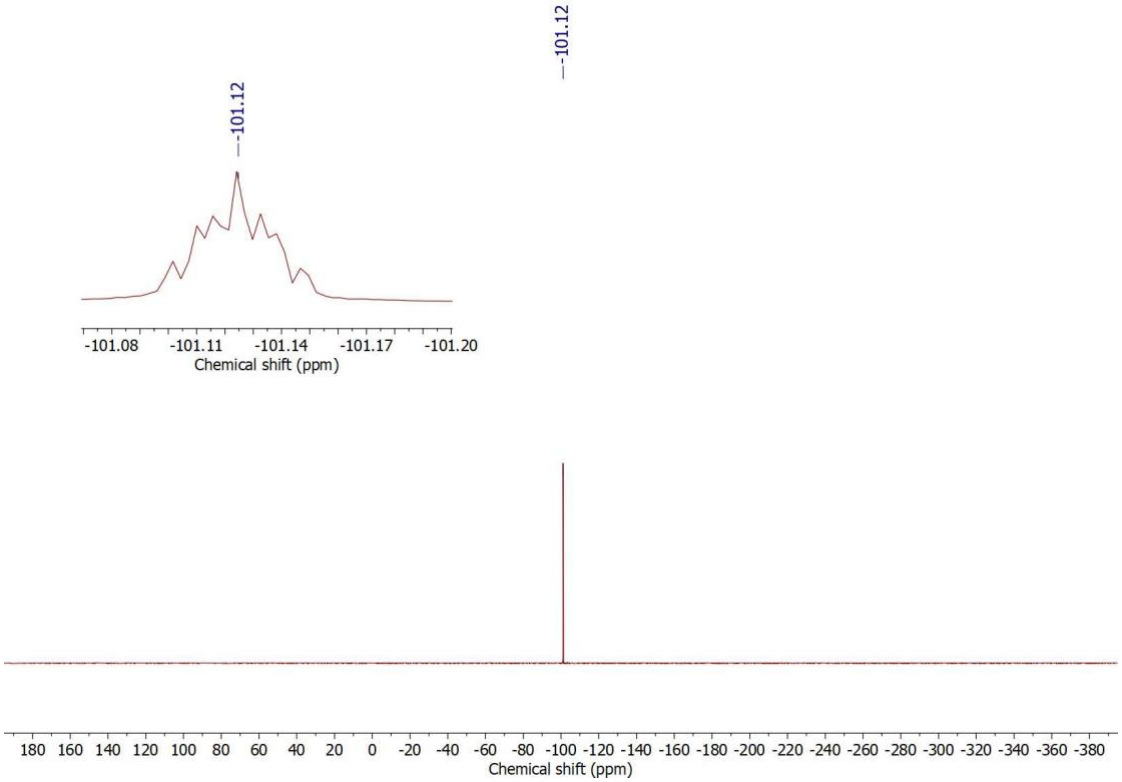

Figure S34: ^{19}F NMR spectrum of [Re(NPhF)Cl_3(CNAr^{Mes2})$_2$] (**7**) in CD_2Cl_2.

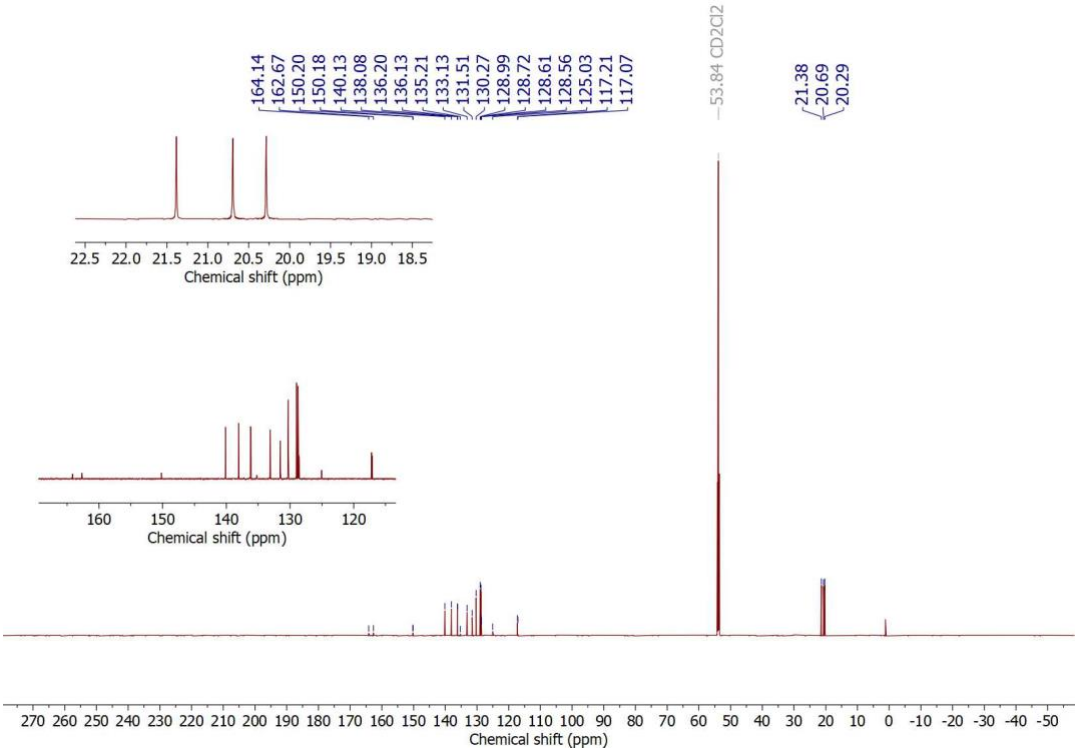

Figure S35: ^{13}C{^{1}H} NMR spectrum of [Re(NPhF)Cl_3(CNAr^{Mes2})$_2$] (**7**) in CD_2Cl_2.

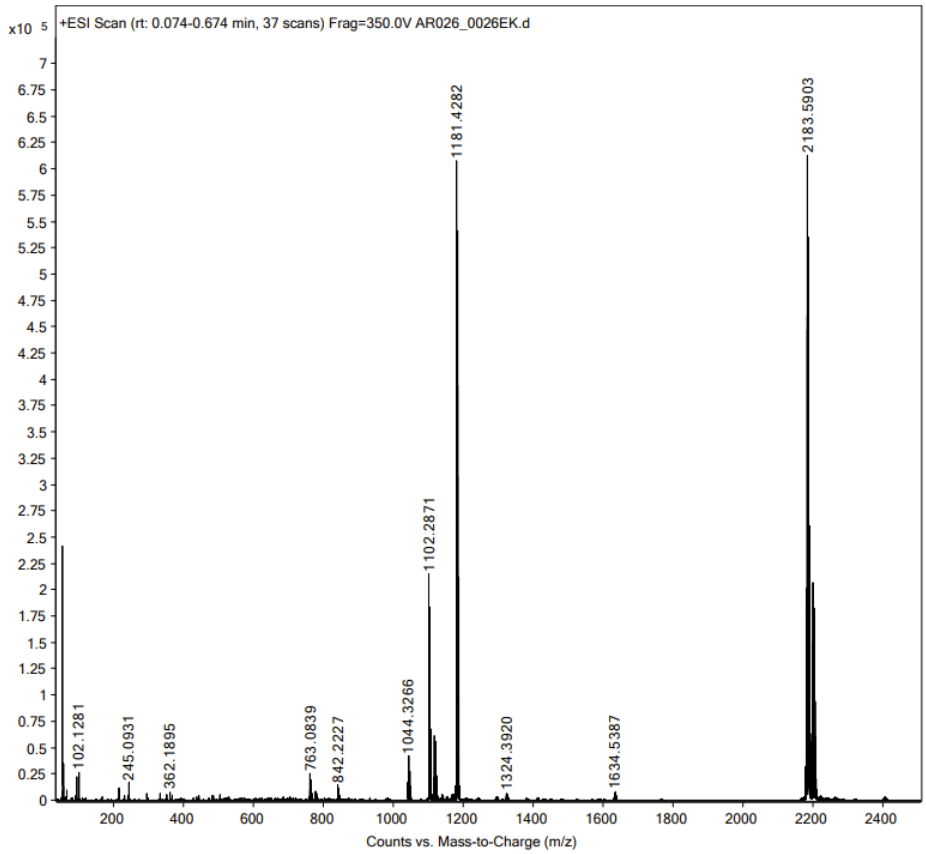

Figure S36: ESI+ mass spectrum of [Re(NPhF)Cl_3($CNAr^{Mes2}$)$_2$] (**7**) in MeCN.

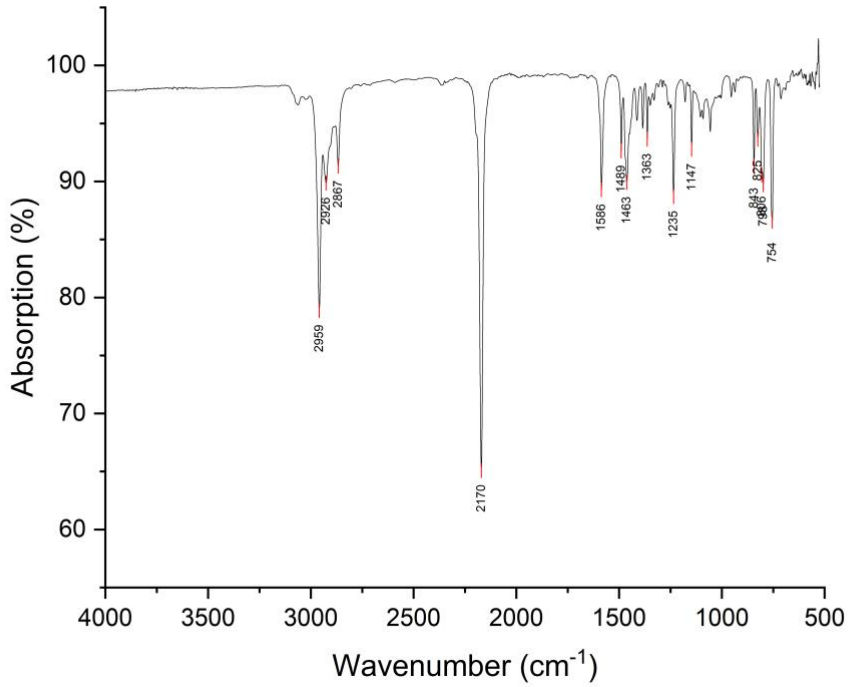

Figure S37: IR (ATR) spectrum of [Re(NPhF)Cl_3($CNAr^{Dipp2}$)$_2$] (**8**).

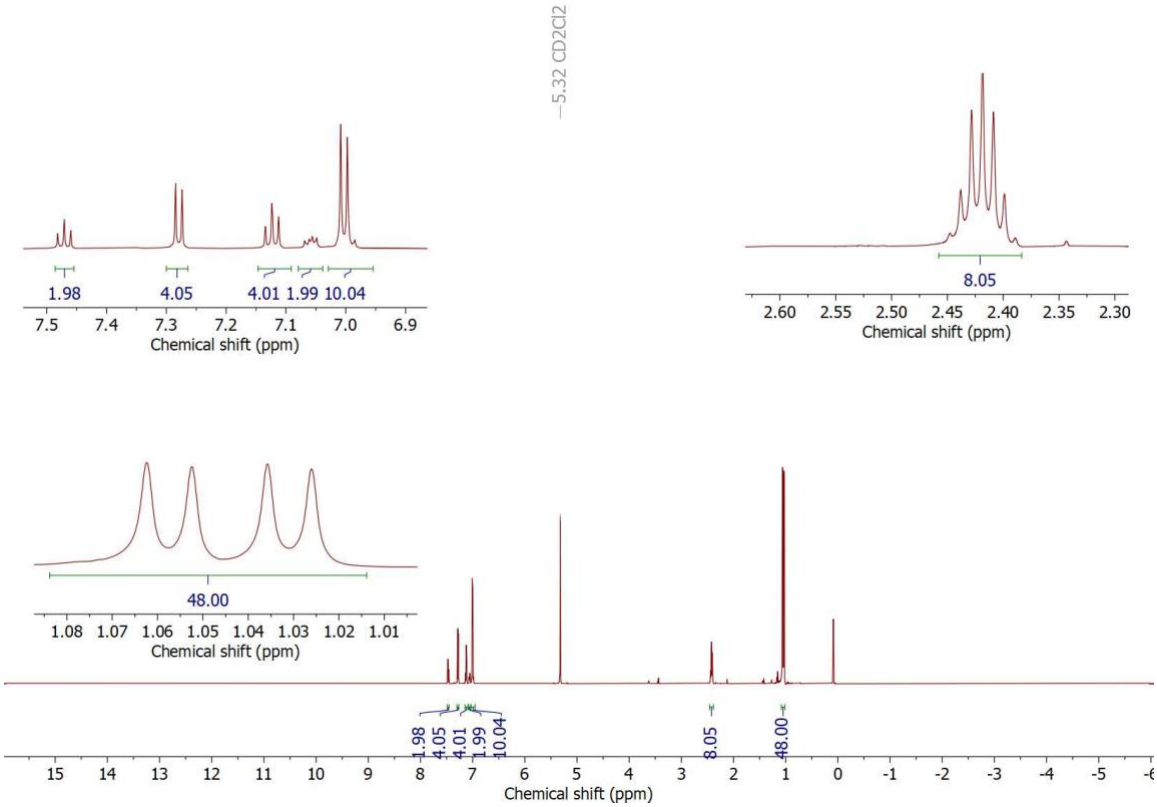

Figure S38: ^{1}H NMR spectrum of [Re(NPhF)Cl$_3$(CNAr^{Dipp2})$_2$] (**8**) in CD$_2$Cl$_2$.

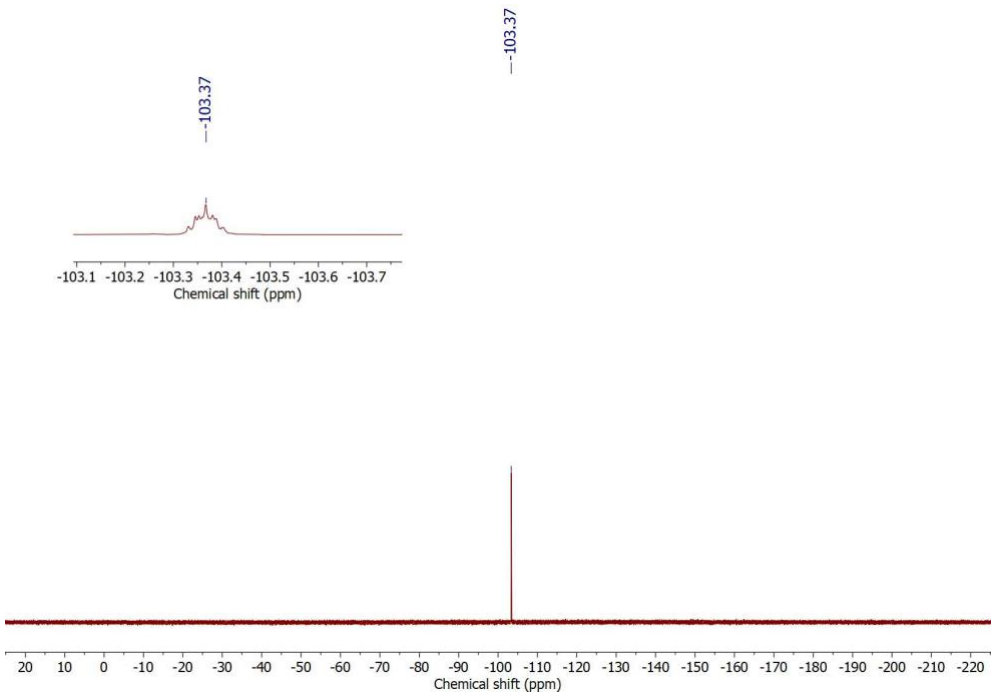

Figure S39: ^{19}F NMR spectrum of [Re(NPhF)Cl$_3$(CNAr^{Dipp2})$_2$] (**8**) in CD$_2$Cl$_2$.

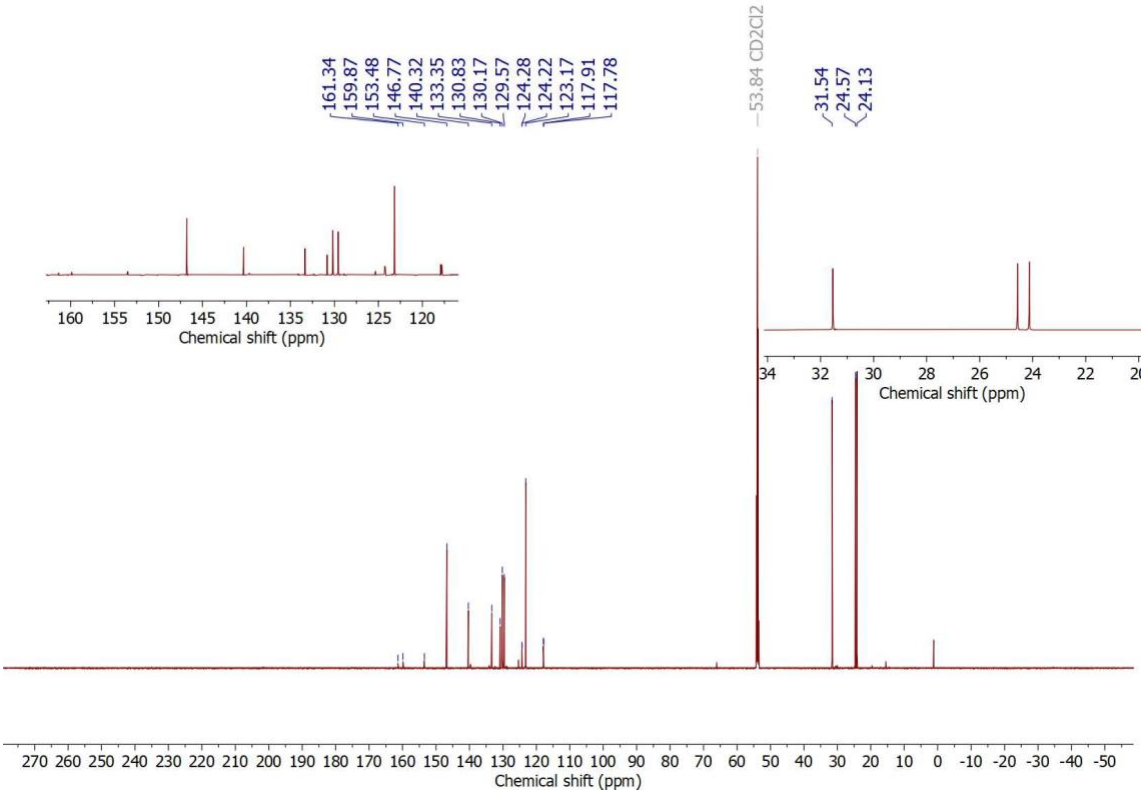

Figure S40: $^{13}C\{^{1}H\}$ NMR spectrum of $[Re(NPhF)Cl_3(CNAr^{Dipp2})_2]$ (**8**) in CD_2Cl_2.

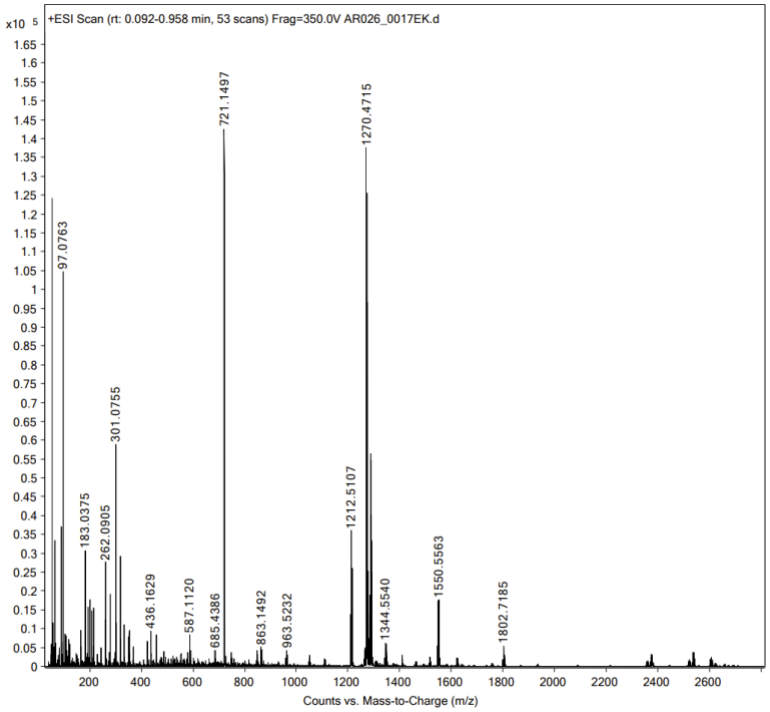

Figure S41: ESI+ mass spectrum of $[Re(NPhF)Cl_3(CNAr^{Dipp2})_2]$ (**8**) in MeCN.

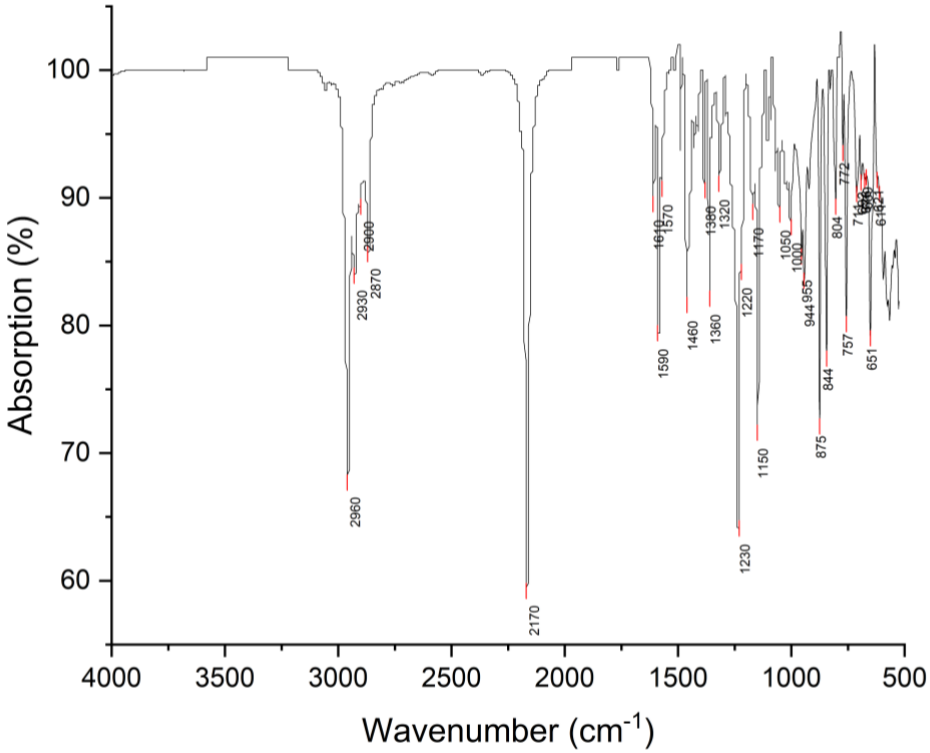

Figure S42: IR (ATR) spectrum of $[Re(NPhF)Cl_3(CNAr^{Tripp2})_2$

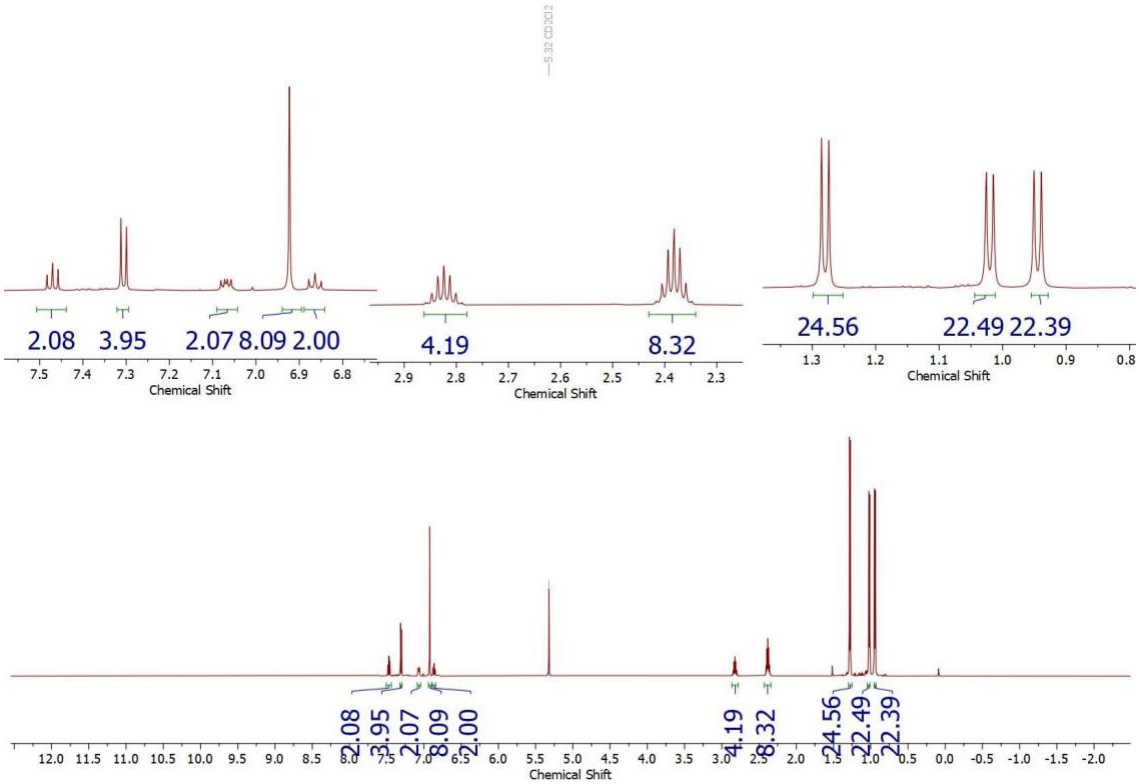

Figure S43: ^{1}H NMR spectrum of $[Re(NPhF)Cl_3(CNAr^{Tripp2})_2]$ (**10**) in CD_2Cl_2.

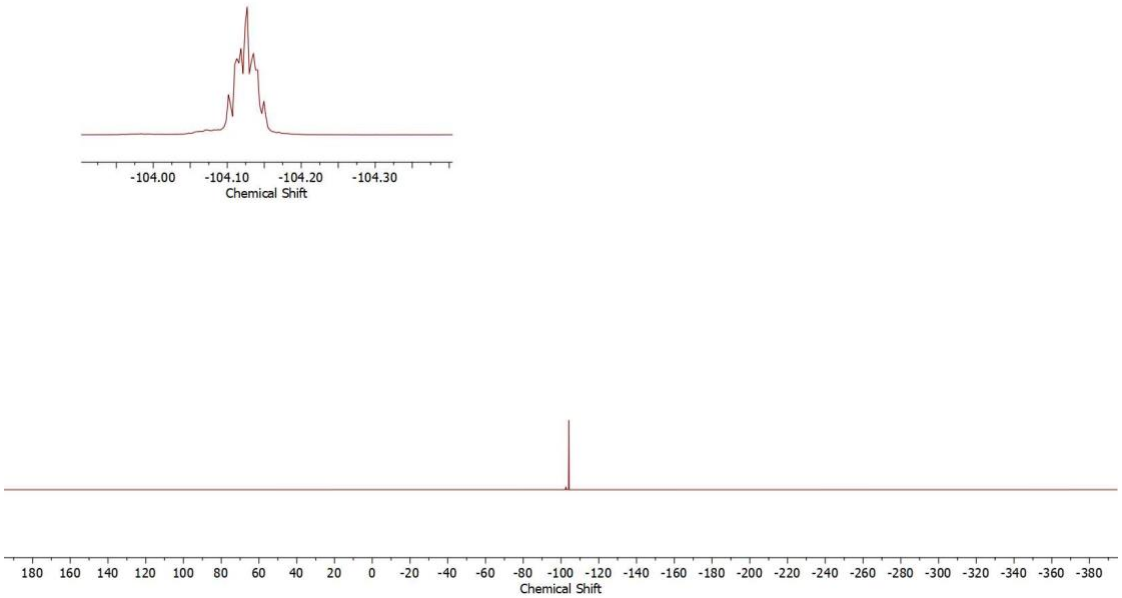

Figure S44: ^{19}F NMR spectrum of [Re(NPhF)Cl$_3$(CNAr^{Tripp2})$_2$] (**10**) in CD$_2$Cl$_2$.

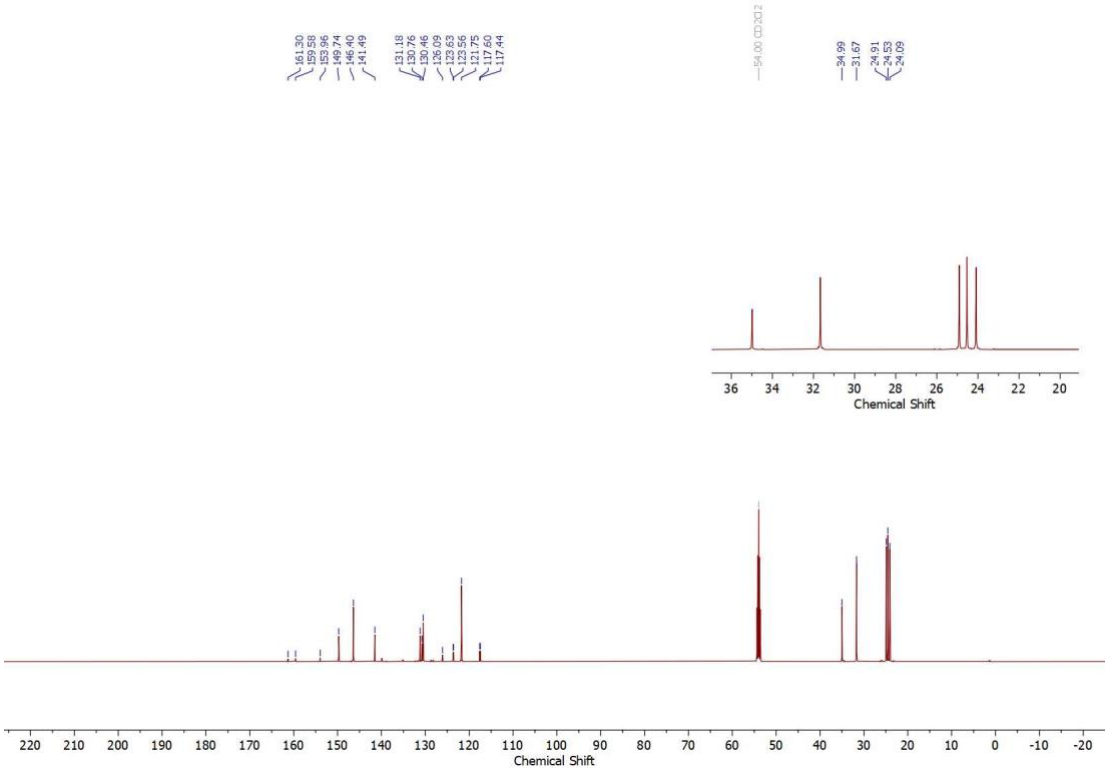

Figure S45: ^{13}C{^{1}H} NMR spectrum of [Re(NPhF)Cl$_3$(CNAr^{Tripp2})$_2$] (**10**) in CD$_2$Cl$_2$.

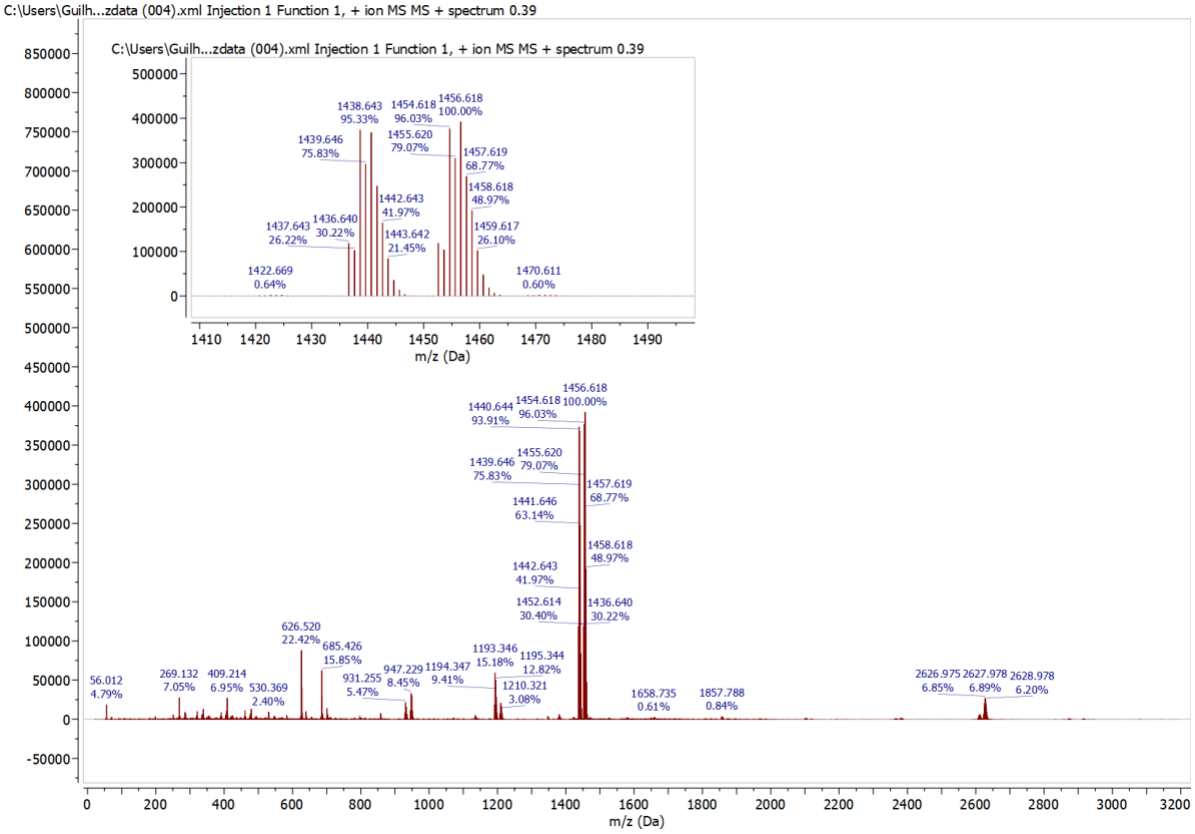

Figure S46: ESI+ mass spectrum of [Re(NPhF)Cl_3(CNAr^{Tripp2})$_2$] (**10**) in MeCN.

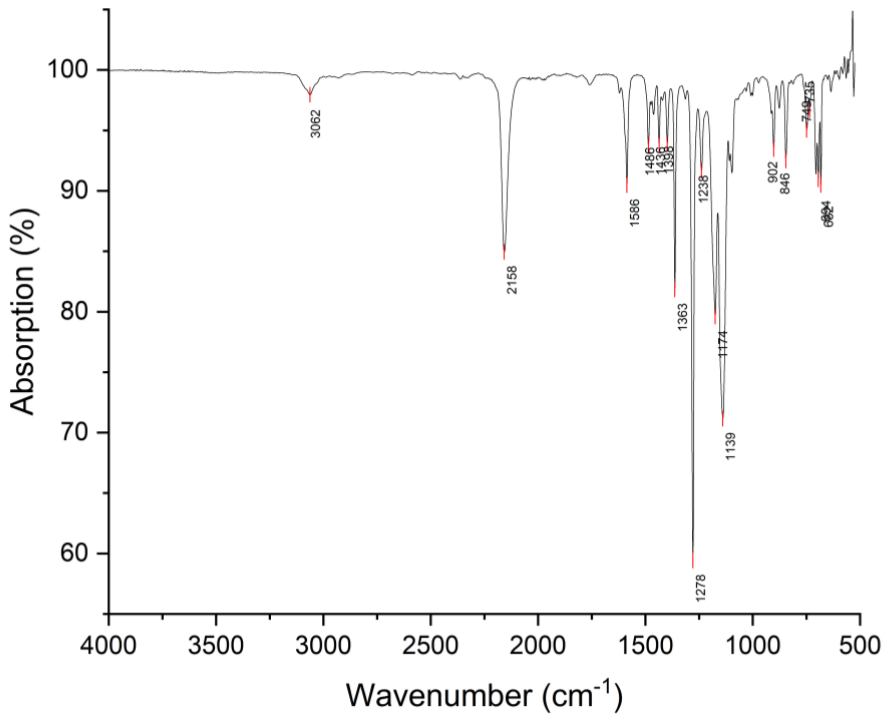

Figure S47: IR (ATR) spectrum of [Re(NPhF)Cl_3(PPh_3)(CNp-FAr^{DarF2})] (**11**).

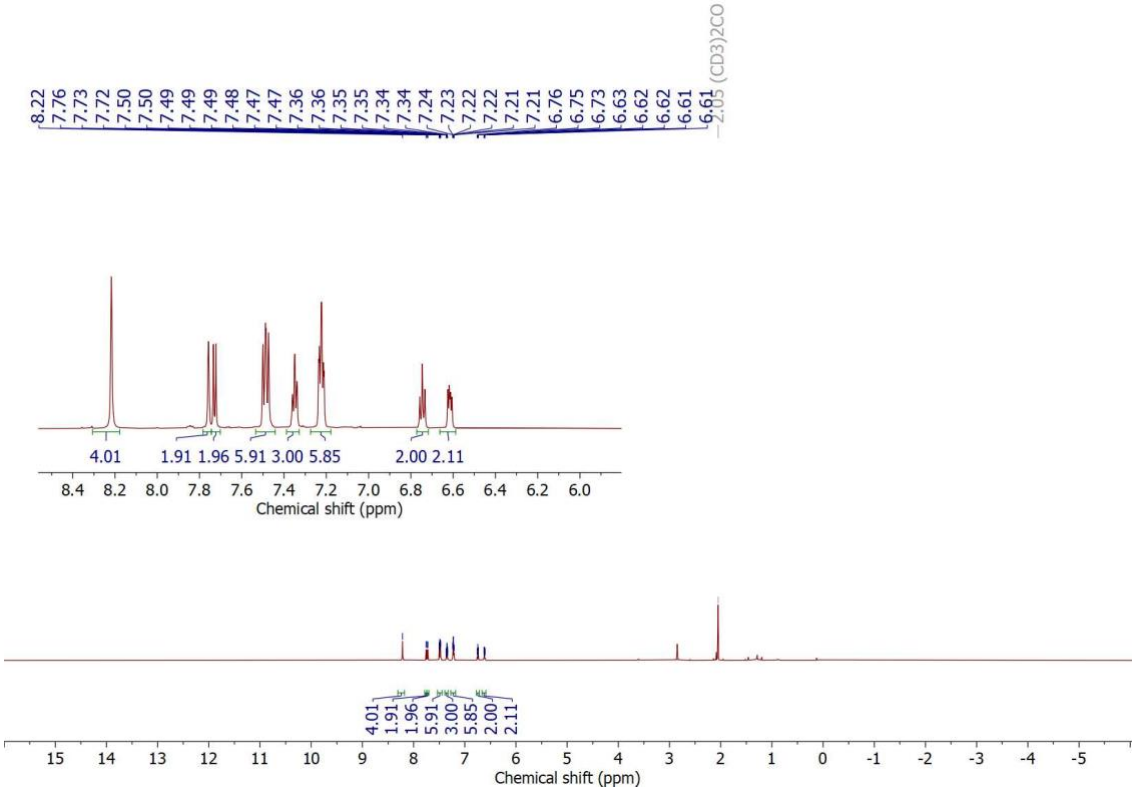

Figure S48: ^{1}H NMR spectrum of [Re(NPhF)Cl$_3$(PPh$_3$)(CNp-FAr^{DarF2})] (**11**) in acetone-d$_6$.

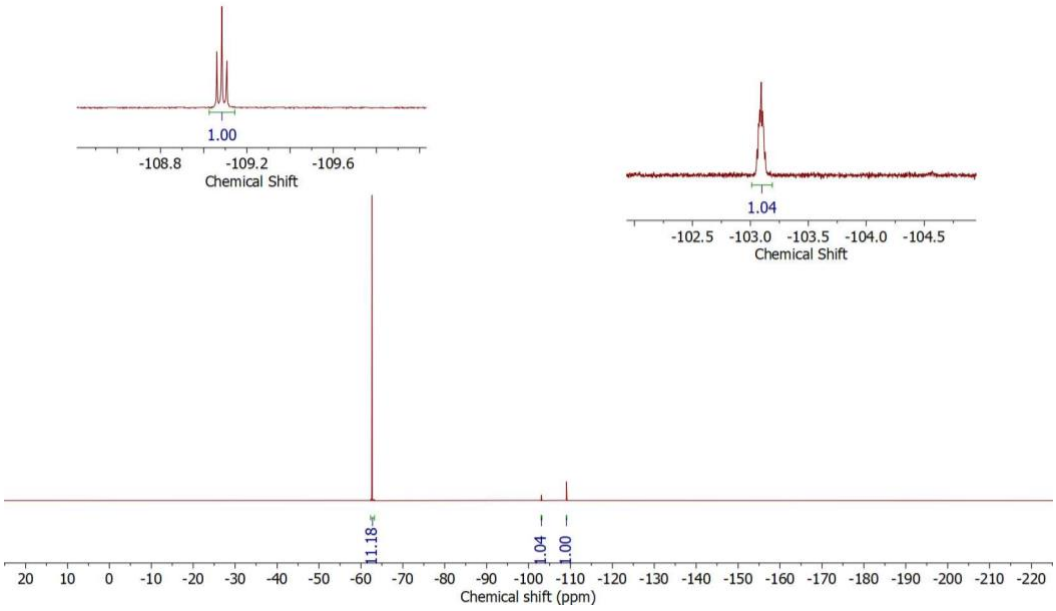

Figure S49: ^{19}F NMR spectrum of [Re(NPhF)Cl$_3$(PPh$_3$)(CNp-FAr^{DarF2})] (11) in acetone-d$_6$.

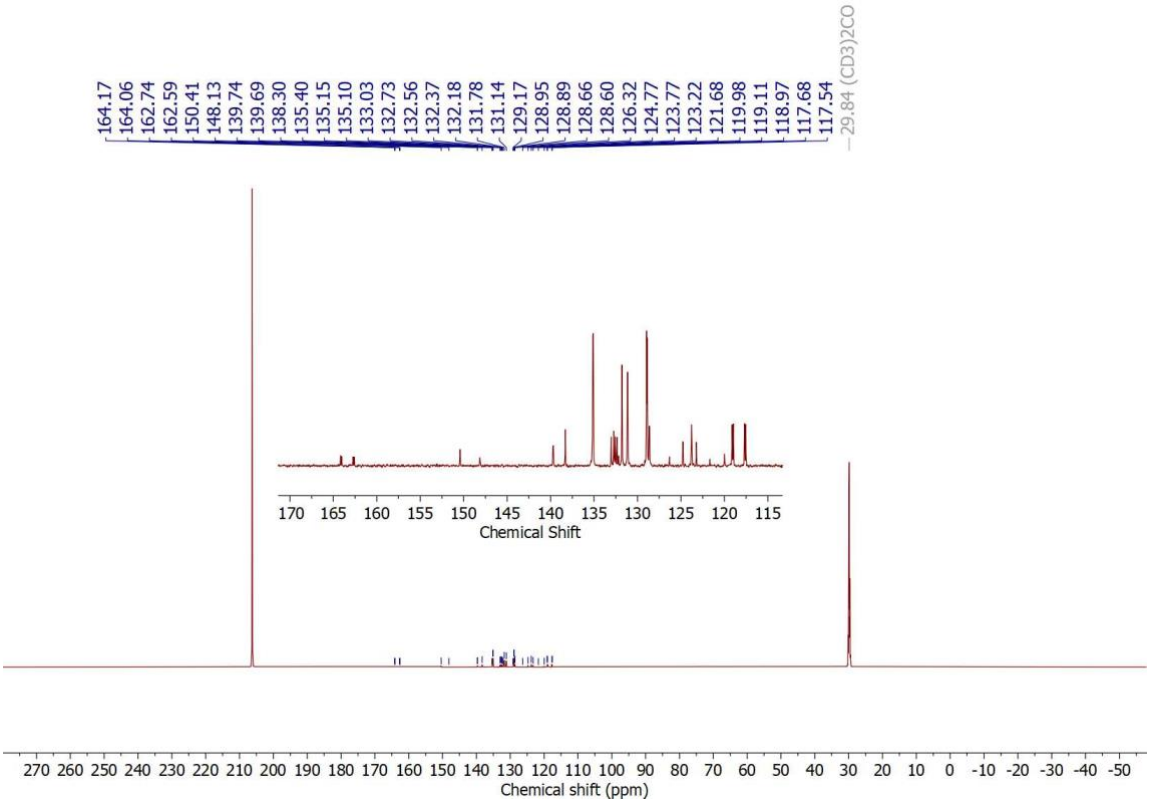

Figure S50: $^{13}C\{^{1}H\}$ NMR spectrum of $[Re(NPhF)Cl_3(PPh_3)(CNp\text{-}FAr^{DarF2})]$ (**11**) in acetone-d_6.

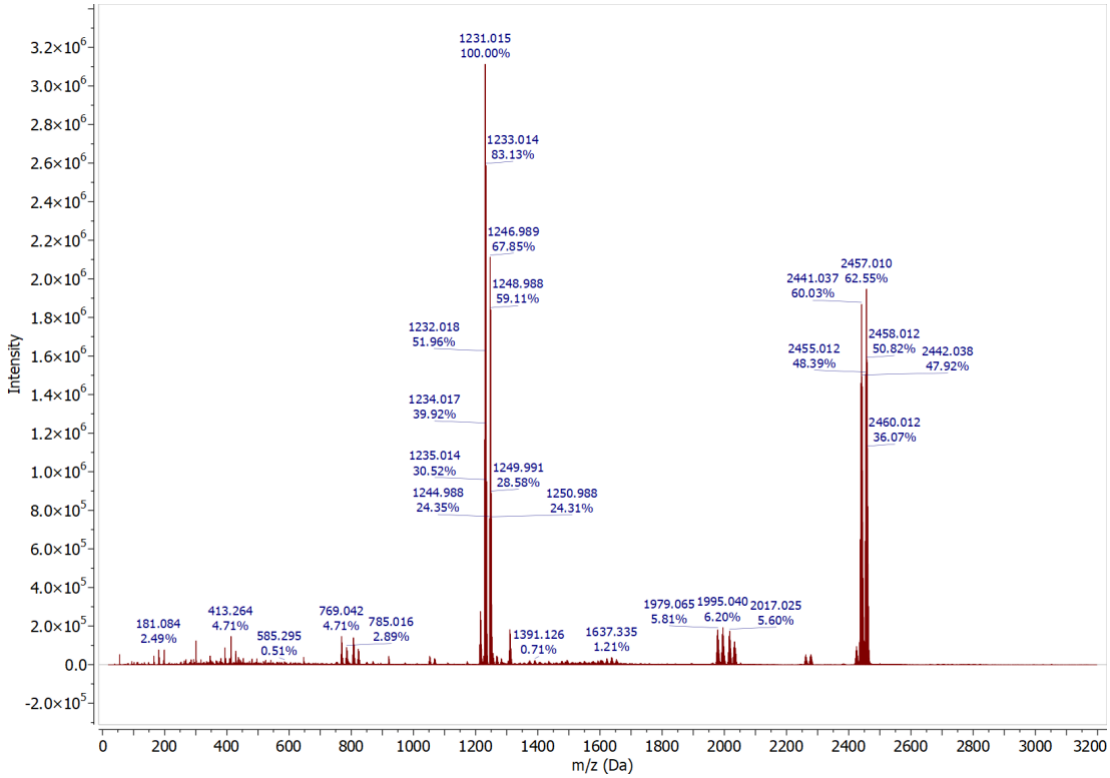

Figure S51: ESI+ mass spectrum of $[Re(NPhF)Cl_3(PPh_3)(CNp\text{-}FAr^{DarF2})]$ in MeCN (**11**).

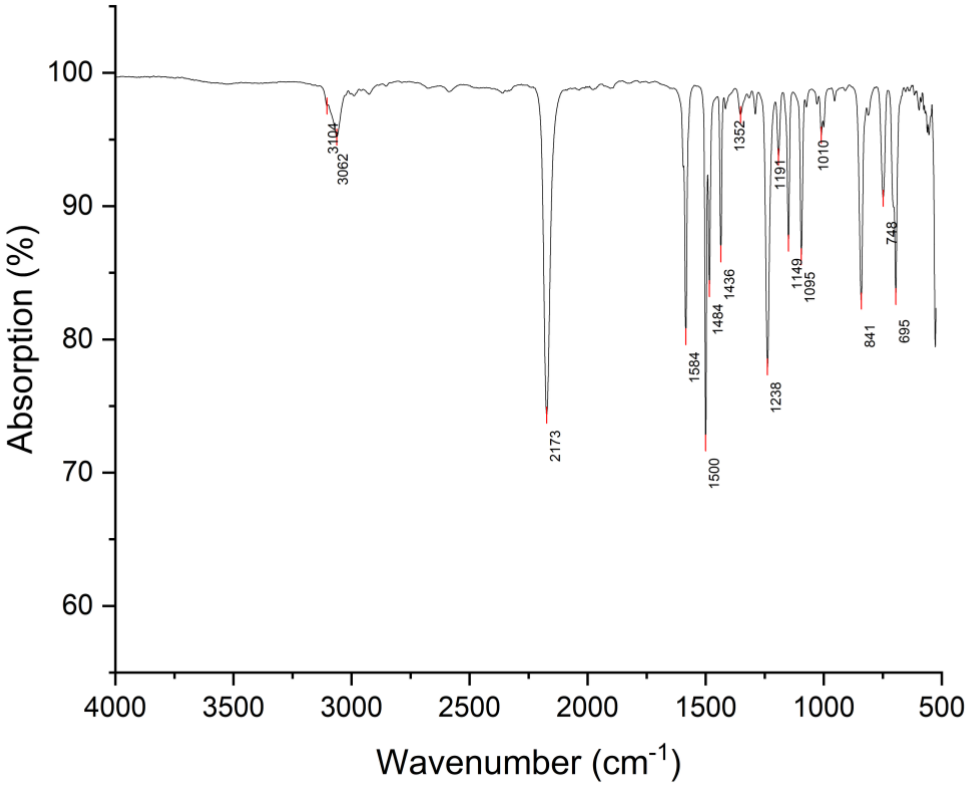

Figure S52: IR (ATR) spectrum of [Re(NPhF)Cl_3(PPh_3)($CNPh^{pF}$)] (**12**).

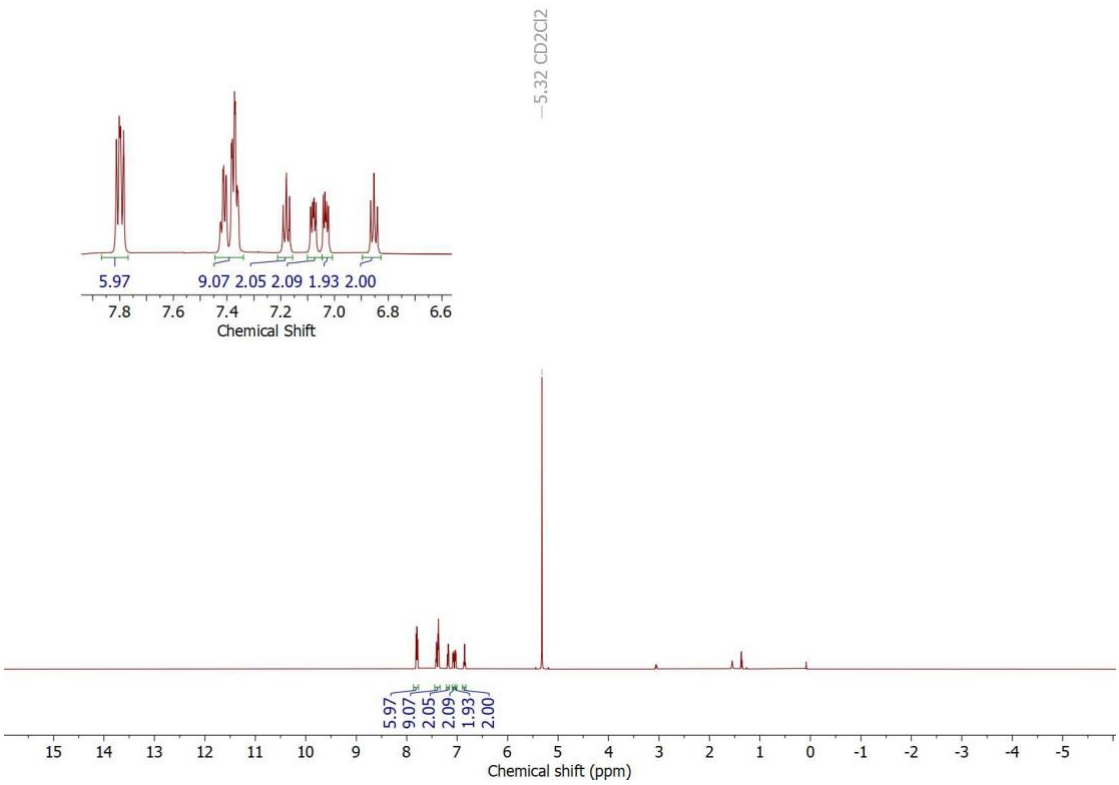

Figure S53: ^{1}H NMR of [Re(NPhF)Cl_3(PPh_3)($CNPh^{pF}$)] (**12**) in CD_2Cl_2.

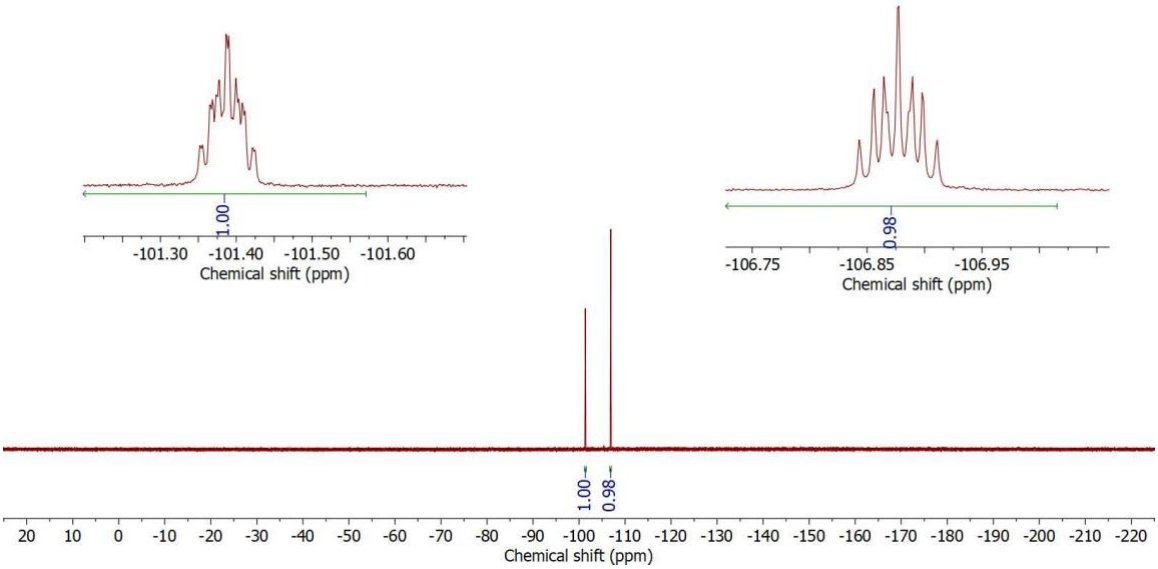

Figure S54: ^{19}F NMR of [Re(NPhF)Cl_3(PPh_3)(CNPh^{pF})] (**12**) in CD_2Cl_2.

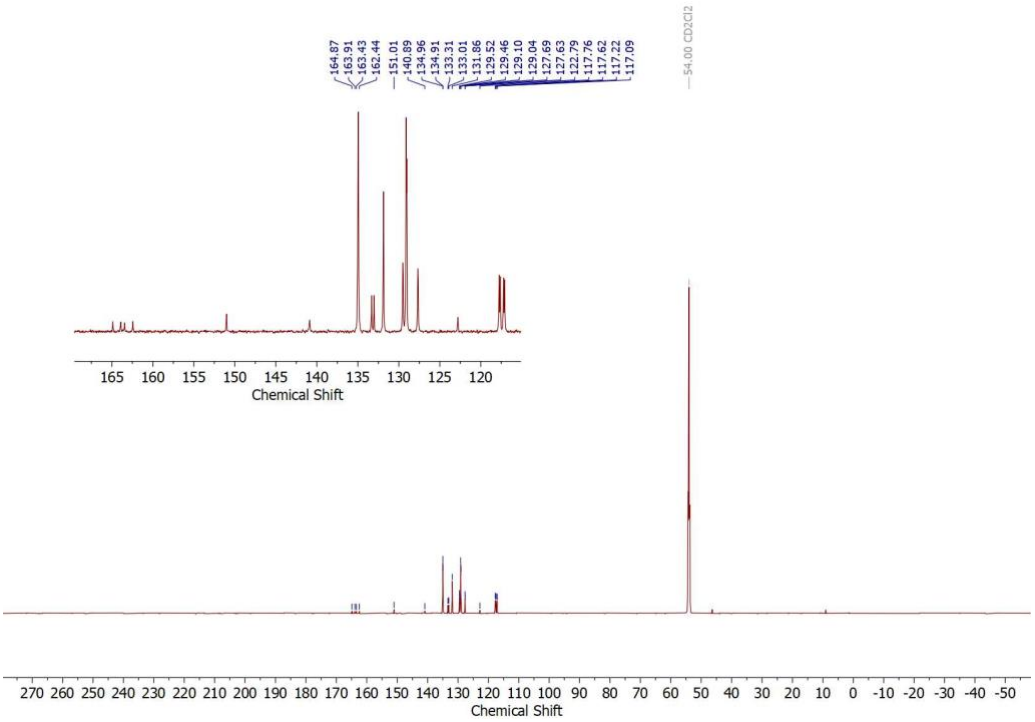

Figure S55: ^{13}C{^{1}H} NMR of [Re(NPhF)Cl_3(PPh_3)(CNPh^{pF})] (**12**) in CD_2Cl_2.

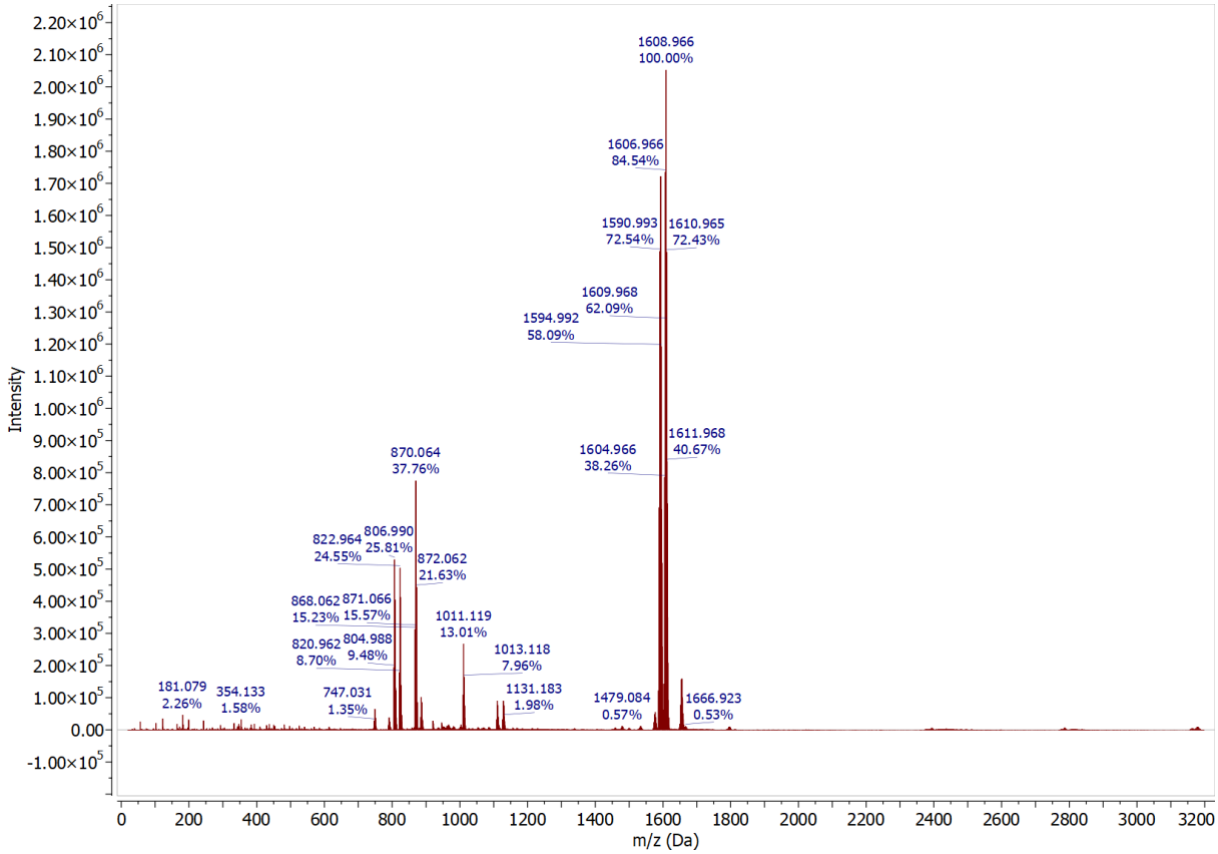

Figure S56: ESI+ mass spectrum of [Re(NPhF)Cl_3(PPh_3)($CNPh^{pF}$)] (**12**) in MeCN.

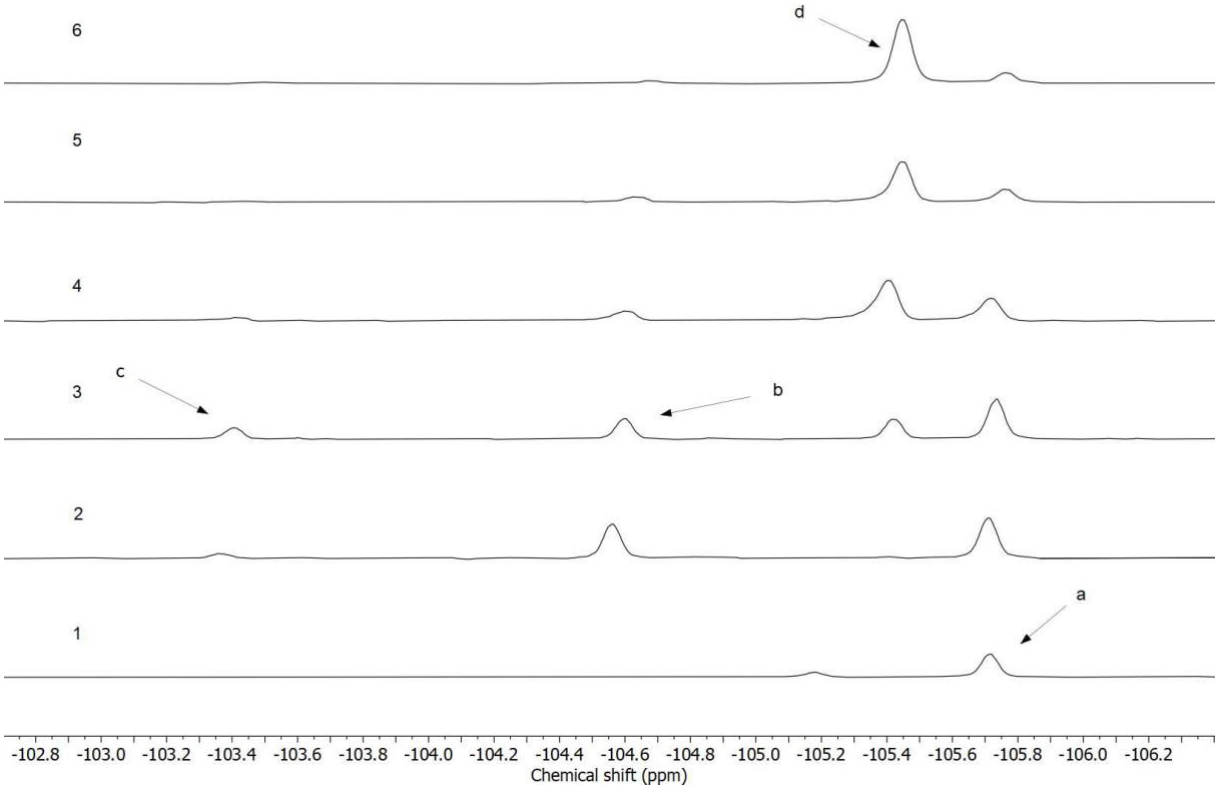

Figure S57: ^{19}F NMR monitoring of reaction of $[Re(NPhF)Cl_3(PPh_3)_2]$ with $CNAr^{Tripp2}$ in a boiling toluene/acetonitrile mixture (5:1). **1** was recorded after 5 minutes, **2** after 1.5 h, **3** after 3.5 h, **4** after 5 h, **5** after 10h, **6** after 13h. As no significant different was observed between **5** and **6**, the heating was not continued. (a: $[Re(NPhF)Cl_3(PPh_3)_2]$; b: $[Re(NPhF)Cl_3(PPh_3)(CNAr^{Tripp2})]$; c: minor intermediate compound, probably $[Re(NPhF)Cl_3(PPh_3)_2(CNAr^{Tripp2})]$; d: $[Re(NPhF)Cl_3(CNAr^{Tripp2})_2]$).

Computational chemistry

As a simple descriptor for the overall donor/acceptor properties of the isocyanides, we determined the quotient from a sum parameter containing the calculated potential energy extrema and the averaged potential energy on the Van der Waals surface of the carbon donor atoms (kcal/mol), and the exposed VdW surface area (Å^2): the **S**urface-**A**veraged **D**onor **A**tom **P**otential (**SADAP**) (Equ. 1). The results for the isocyanides discussed in the present study are summarized in Table 2. The derived sum parameter corresponds to the average interaction energy of the isocyanide carbon atom with positively and negatively charged moieties over its entire accessible surface.[5]

$$SADAP = \frac{EP_{min}+EP_{max}+AP}{ES_{pos}+ES_{neg}} \qquad \text{(Equ.1)}$$

Table S13. Calculated electrostatic potential surface properties of the isocyanide carbon atom at the Van der Waals (VdW) boundary for structures optimized at the B3LYP/6-311++G** level. Surface properties were evaluated at ρ = 0.001 level using an electrostatic potential map basis with a grid-point spacing of 0.25. The last column contains the Surface-Averaged Donor Atom Potential SADAP = (EP_{min} + EP_{max} + AP)/(ES_{pos} + ES_{neg}) as a combined descriptor of steric and electrostatic properties of the potential ligands, which allows an estimation of their reactivity.[5]

CN-R	Exposed VdW surface, ES (Å^2)		Extrema for potential energies at VdW surface, EP (kcal/mol)		Average potential energies at VdW surface, AP (kcal/mol)	Surface-averaged donor atom potential SADAP, (kcal/mol Å^2)
R =	ES_{pos}	ES_{neg}	EP_{min}	EP_{max}	$\varnothing_{overall}$	SADAP
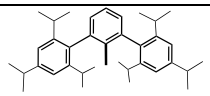 CNAr^{TRIPP2}	0.00	22.23	-38.01	-9.31	-26.65	-3.33
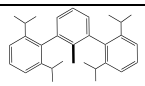 CNAr^{Dipp2}	0.00	22.13	-37.64	-8.87	-26.04	-3.28
 CNPh$^{i\text{-}prop2}$	0.00	25.99	-35.47	-5.16	-21.20	-2.38
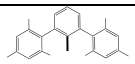 CNAr^{Mes2}	0.00	30.10	-39.20	-7.01	-25.11	-2.37
 CNMes	0.00	28.89	-36.79	-6.83	-21.68	-2.26
 CN^{t}Bu	0.00	31.43	-39.63	-5.86	-22.00	-2.15

 CNPh	0.05	31.28	-35.20	1.72	-18.01	-1.64
 CNPh$^{p\text{-}F}$	1.67	29.53	-32.02	7.05	-14.10	-1.25
 CNPh$^{p\text{-}NO2}$	6.15	24.86	-28.59	9.44	-10.27	-0.95
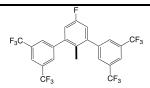 CNp-FAr^{DArF2}	20.50	6.74	-11.49	69.07	16.88	2.73

References

1. P. Coppens, *The Evaluation of Absorption and Extinction in Single-Crystal Structure Analysis. Crystallographic Computing*; Copenhagen, Muksgaard, **1979**.
2. G. M. Sheldrick, A short history of SHELX. *Acta Crystallogr*. 2008, **64**, 112–122.
3. G. M. Sheldrick, Crystal structure refinement with SHELXL. *Acta Crystallogr*. 2015, **71**, 3–8.
4. H. Putz, K. Brandenburg, *DIAMOND, Crystal and Molecular Structure Visualization,* Crystal Impact; Version 4.6.5; GbR: Bonn, Germany, **2021**.
5. G. Claude, J. Genz, D. Weh, M. Roca Jungfer, A. Hagenbach, M. Gembicky, J. S. Figueroa and U. Abram, *Inorg. Chem*. 2022, **61**,16163-16176.